



Università degli Studi di Ferrara

**DOTTORATO DI RICERCA IN
BIOCHIMICA, BIOLOGIA MOLECOLARE E
BIOTECNOLOGIE**

COORDINATORE PROF. FRANCESCO BERNARDI

**MOLECULAR MECHANISM AND RNAi CORRECTION OF A
DOMINANT-NEGATIVE VON WILLEBRAND FACTOR
GENE DELETION**

DOTTORANDA

DOTT.SSA CATERINA CASARI

TUTORE

DOTT. MIRKO PINOTTI
PROF. FRANCESCO BERNARDI

XXII° CICLO

ANNI 2007 - 2009

*To my family and my nephews,
to my best friends,
most important people in my life.*

CONTENTS

LIST OF ABBREVIATIONS	3
INTRODUCTION.....	4
- VON WILLEBRAND FACTOR IN HAEMOSTASIS AND COAGULATION.....	5
- VON WILLEBRAND FACTOR SYNTHESIS AND STRUCTURE...	7
- VON WILLEBRAND DISEASE.....	12
• VWD 2A subtypes IIC, IID and IIE/F	14
- RNA-INTERFERENCE: CORRECTION APPROACH TO DOMINANT DISEASES.....	16
BACKGROUND INFORMATION OF THE p.P1105_C1926delinsR GENE DELETION AND OUTLINE OF THIS THESIS.....	20
MATERIAL & METHODS.....	24
• Creation of expression vectors	25
• Expression of recombinant VWF in eukaryotic cells	27
• Silencing	27
• mRNA study	29
• Antibodies	30
• Analysis of recombinant VWF	30
• Immunofluorescence microscopy	31
RESULTS.....	33
• Creation of the deleted expression vector	34
• Expression of the in-frame deleted VWF	36
• Dominant-negative effect of the VWF deletion – cellular model	38
• Interfering with dimerization of the in-frame deleted protein by a natural mutation affecting VWF dimerization (C2773R)	45

• Interfering with dimerization of the in-frame deleted protein by RNA silencing - Correction strategy	47
GENERAL DISCUSSION.....	51
REFERENCES.....	56
ABSTRACT.....	69
RIASSUNTO IN ITALIANO.....	70
<i>Curriculum vitae & Acknowledgement</i>	71

LIST OF ABBREVIATIONS:

CK - "cysteine knot" domain
dsRNA - double stranded RNA
ER - Endoplasmic Reticulum
FVIII - factor VIII
HMWM - high molecular weight multimer
LMWM - low molecular weight multimer
PC - pachyonychia congenita
PCR - polymerase chain reaction
pDEL - (pP1105_C1926delinsR) expression vector for the deleted VWF
pDEL/C2773R - expression vector for the double mutant VWF
pWT - (pSVHVWF) expression vector for wild type VWF (with mutated SacI restriction site at position 8876)
RISC - RNA-induced silencing complex
RNAi - RNA interference
RT - reverse transcription
shRNA - short hairpin RNA
siRNA - short interfering RNA
TTP - thrombotic thrombocytopenic purpura
UTR - untranslated region
WPB - Weibel-Palade body
VWD - von Willebrand diseases
VWF - von Willebrand factor
VWF:Ag - von Willebrand factor antigen assay
VWF:CB - von Willebrand factor collagen-binding activity
wt - wild type

INTRODUCTION

VON WILLEBRAND FACTOR IN HAEMOSTASIS AND COAGULATION

Haemostasis is a tightly regulated and dynamic process that maintains the integrity of the mammalian circulatory system under normal conditions. The ultimate goal is to maintain the blood in a fluid state within the vascular compartment but allowing it to coagulate in case of trauma. It refers to the complex interaction between vessels, blood cells, coagulation factors, coagulation inhibitors and fibrinolytic proteins.

In the resting state the integrity of blood vessels allows endothelial cells to inhibit platelet adhesion/activation and thus blood coagulation's starting. In addition, the synthesis of anticoagulant proteins (as activated protein C) was continuously promoted by the presence of basal levels of procoagulant molecules: the maintenance of this equilibrium prevent clots formation¹.

After vessel injury, the balance between these processes is disturbed, and quick, localized and subtle regulated events occur to restore the equilibrium.

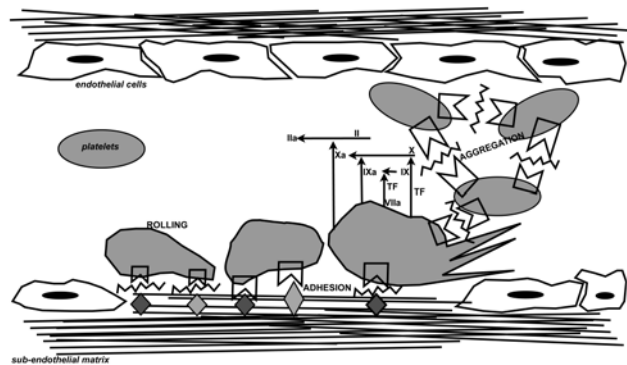


Figure 1: Schematic overview representation of processes that occur after vessel injury, in which VWF is actively involved.

First, vasoconstriction narrows the blood vessel thereby minimizing the vessel diameter and slowing bleeding.

Damaged endothelial cells display negatively charged phospholipids and release procoagulant proteins², underlying tissue exposes collagen allowing platelets to adhere and aggregate in the primary hemostatic plug that temporarily blocks blood loss³. Consequently platelets were made active and the coagulation cascade is initiated and amplified at each step finally producing fibrin, which is responsible of the platelet plug stabilization⁴.

After vessel repair, fibrinolysis results in fibrin, and thus clot, dissolvment^{5,6}.

In these regulated series of events, a major role is held by VWF. This multimeric glycoprotein circulates in plasma in a globular, inactive state but, at site of vascular injury, the high shear stress and subendothelial matrix exposition convert VWF into its active conformation, which allows platelet adhesion and aggregation. Since platelets are unable to bind to matrix components in high shear stress condition in the absence of VWF⁷, the bridge-function of VWF is essential for the platelet plug formation.

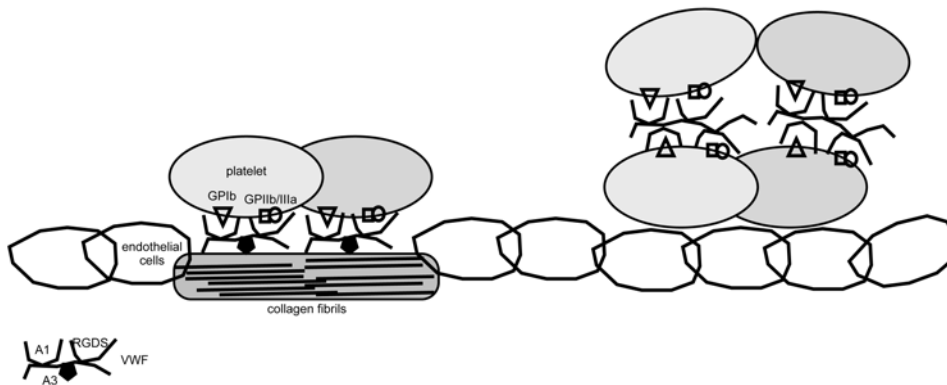


Figure 2: Easy description of major roles of VWF in platelet plug formation. First (left) VWF binds to sub-endothelial collagen exposed after vessel injury and allow platelet rolling and adhesion. Subsequently VWF allow platelet aggregation (right) and thrombus formation.

The VWF carries another important function, related to the maintenance of the haemostasis, as carrier of FVIII⁸⁻¹⁰ that is an important and essential factor involved in the coagulation cascade¹¹. VWF-FVIII complex formation prevents premature clearance of FVIII from circulation^{11,12}.

VON WILLEBRAND FACTOR: BIOSYNTHESIS & STRUCTURE

VWF is synthesized by endothelial cells and megakaryocytes^{13,14}. VWF gene (178 kb) is located on the short arm of chromosome 12 (12p13.3)^{7,15,16} and a not functional pseudogene (21-29 kbp) partially overlapping with full-length gene (exons 23-34) is situated on chromosome 22q11.1^{17,18}.

The primary mRNA (9 kb) product (52 exons) is first translated in a single pre-pro-polypeptide chain of 2813 amino acids and include a signal peptide (22 residues), a large pro-peptide (741 residues) and the mature subunit of 2050 residues (Figure 3). Almost entire pro-protein (>90%) has highly repetitive structure and is composed of four types (A-D) of repeated domains shared with others proteins (integrins, components of the complement system, thrombospondin and collagens). These motifs are arranged in the sequence: D1-D2-D'-D3-A1-A2-A3-D4-B1-B2-B3-C1-C2-CK⁷.

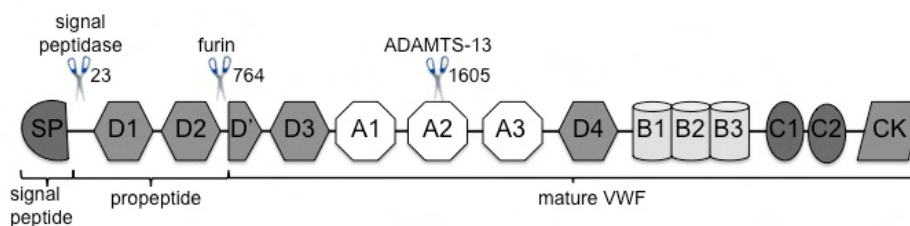


Figure 3: Schematic representation of the pre-pro-VWF domain organization. Scissors indicate sites where VWF is cleaved during synthesis (before Ala23-signal peptidase site of cleavage- and Ser764 - furin site of cleavage-) or in plasma in the A2 domain (after Tyr1605 - ADAMTS-13 site of cleavage-). The diagram is not on scale.

It is remarkable that 234 residues (8.3%) of the preproVWF are cysteine, which are abundantly clustered in the amino and carboxyl terminal region and rare in the A motifs. In the secreted VWF all Cys are paired in intra- or inter-molecular disulfide bonds.

The mature subunit is extensively glycosylated (12 N-linked and 10 O-linked oligosaccharides)⁷.

Formation of large VWF multimers is a complex and thinly regulated series of events (Figure 4).

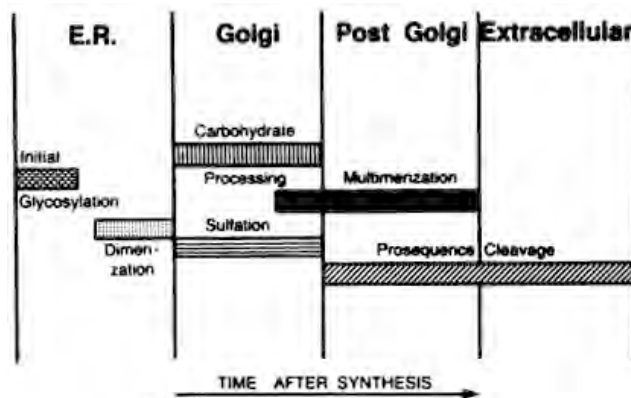


Figure 4: Schematic representation reported by Wagner DD et al¹⁹ that indicate the biosynthetic steps of VWF synthesis and the cellular compartment where they occur.

After removal of the signal peptide by a signal peptidase, proVWF is translocated to the endoplasmic reticulum (ER) where it undergoes initial N-linked glycosylation and dimerization¹⁹ (Figure 5). This event occurs through disulfide bond formation between C-terminal “Cysteine Knot” (CK) domain^{7,20-22}. It has been demonstrated that mutations in the Cys2773 (within sequence Cys²⁷⁷¹-Ser-Cys-Cys²⁷⁷⁴) abrogate dimerization²³ and subsequent studies indicate that this residue is involved in the inter-chain disulfide bond with the corresponding residue in a second subunit²⁴.

ProVWF dimers are then transported to the Golgi apparatus where N-linked glycosylation is completed and O-linked glycosylation is applied²⁵ (these modifications add 19% to the weight of the protein)²⁶⁻²⁸. Moving to the trans Golgi network, the furin-mediated²⁹⁻³² pro-peptide (D1-D2 domains) cleavage occurs and, consequently, facilitate the multimerization through D'D3 amino-terminal regions of dimers^{33,34}. Multimers, which can rise 20000 kDa, are designated to constitutive secretion (\approx 95%) or to storage in specialized cellular compartment as rod-shaped Weibel-Palade body (WPB) in endothelial cells and α -granules in platelets³⁵⁻³⁷ (Figure 5-6).

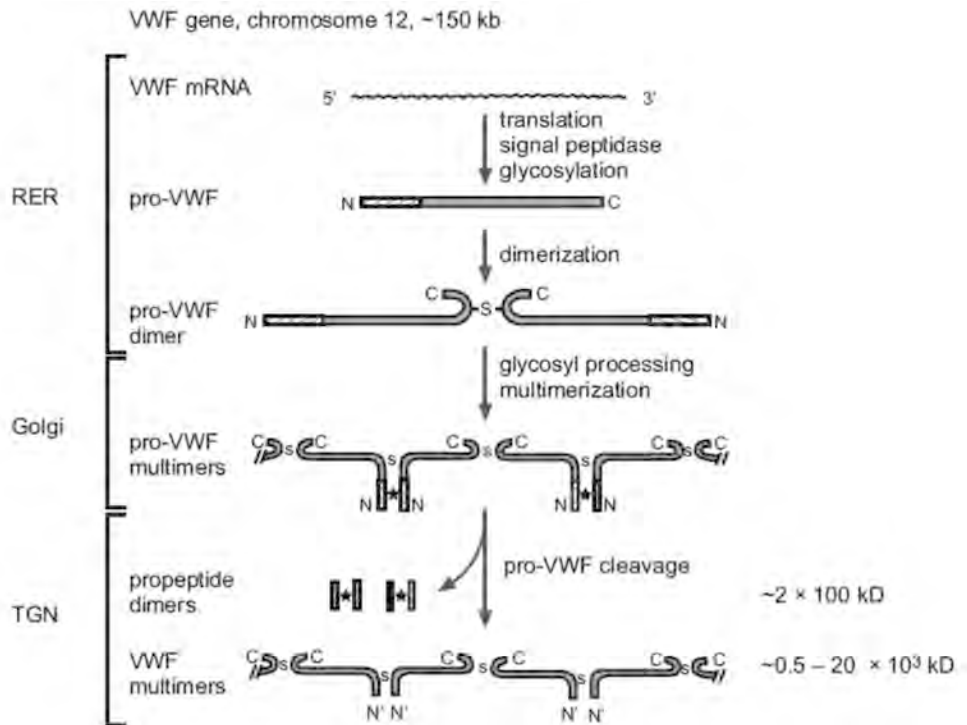


Figure 5: Schematic representation of the processing steps involved in the biosynthesis of von Willebrand factor. ★ = non-covalent interaction; S = disulphide bonds. The molecular mass of the different VWF species is given on the right^{38,39}.

WPBs appear to be composed by longitudinally oriented tubules surrounded by a membrane and multimerization itself is considered the triggering event for WPB-granules formation⁴⁰. The largest polymers, i.e. ultra-large multimers, are internalized and VWF secretion from these storage dispenses are related to secretagogues stimuli. Sorting from granules requires the pro-peptide that function as catalyst in multimerization and as a molecular chaperone in translocation to storage granules. The stoichiometry of the pro-peptide and mature VWF in WPB is 1:1^{19,41,42}. The release of these forms of VWF at sites of vascular damage would deliver the most thrombogenic molecules directly where needed.

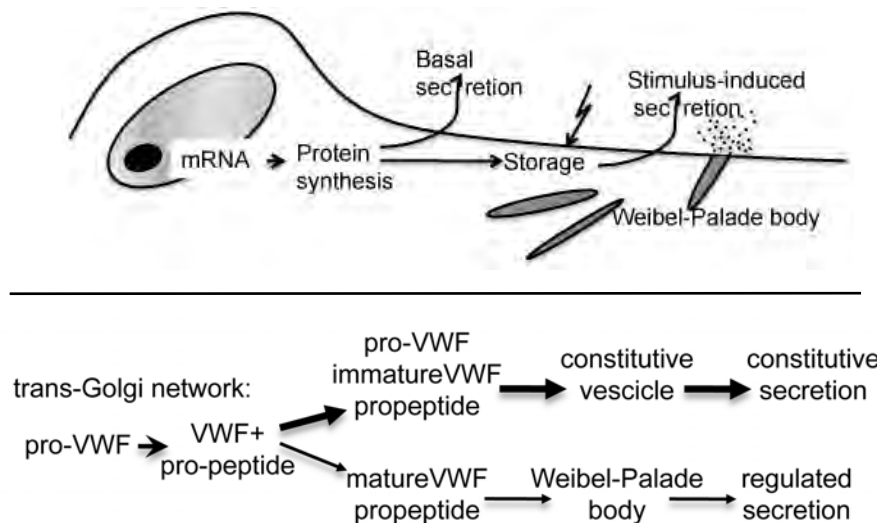


Figure 6: Partitioning of VWF propeptide and pro-VWF between the constitutive and regulated secretory pathway by vascular endothelial cells. The pro-VWF molecule is processed in the trans-Golgi network and results in heterogeneous forms of VWF, ranging from dimers to large polymers. The largest species, consisting of partially processed and immature VWF, is secreted through the constitutive pathway. The remainder, largest, fully processed and functional VWF, is sorted into the Weibel-Palade bodies and secreted via the regulated pathway. This model proposes that the majority of VWF is secreted through the constitutive pathway^{38,39}.

In vivo, VWF and pro-peptide plasma levels are 10 and 1 $\mu\text{g/ml}$, with 12 h and 2 h half-life, respectively. About 66% of total variation in plasma VWF levels is genetically determined and approximately 30% of this genetic component can be explained by ABO blood group. Average VWF plasma levels for persons carrying blood group O are 25% to 35% below that of persons with other blood groups⁴³⁻⁴⁷.

When secreted in blood flow, VWF multimer size is well regulated by the enzymatic activity of a metallo-protease named ADAMTS-13⁴⁸⁻⁵⁰ (Figure 3). A deficiency in the ADAMTS-13 protease activity results in the presence of ultra-large VWF multimers that may cause thrombotic thrombocytopenic purpura⁵¹ (TTP), which is manifested by thrombocytopenia, microangiopathic hemolytic anemia, bleedings and other symptoms⁵². Several VWF domain-specific functions have been identified and elucidated. D domain contains FVIII and heparin binding site and, in addition, D'D3 may contain P-selectin site of interaction. P-selectin appears

to anchor released ultra-large multimers to the surface of activated endothelial cells and contribute to present ADAMTS-13 cleavage site⁵³⁻⁵⁵. A1 domain contains the binding site for platelet receptor GPIb α , heparin, sulphated glycolipids and snake venom botrocetin. It's still controversial if this domain contain also a binding site for collagen⁵⁶. Scientific researchers agree that collagens type I and III binding site are located within the A3 domain. Integrin α II β 3 binds to RGD sequence located within C1 domain. The A2 domain contains the ADAMTS-13 cleavage site. Both the A1 and A3 binding sites and their accessibility seem to be dependent on the fluid dynamic forces exerted on the molecule as well as its immobilization on a surface⁴⁰.

The majority of binding sites for numerous ligand are located within A domains, in accordance to the evolutive properties of this kind of modules, characteristic of adhesive proteins⁵⁷. On the other hand, amino and carboxy-terminal ends are more implicated in the VWF structure determination than in ligand binding.

Neither VWF structure nor its adhesive properties are dispensable to allow all VWF-dependent function at sites of vascular injury. This notion is supported by severe VWD due to mutations in either A and D-C domains.

VON WILLEBRAND DISEASE

Von Willebrand Disease is an inherited bleeding disorder due to deficiency and or dysfunction in von Willebrand factor protein, and is a relatively common cause of bleeding although the precise prevalence is very difficult to estimate ranging between very different values (0.0023%-1,3%)⁵⁸. Considering only VWD due to genetic mutations occurring in the *VWF* genes, there is no evidence for a single major gene rearrangement associated to a large fraction or more severe cases⁵⁸. Since the 1926⁵⁹, when a new bleeding disorder different from haemophilia was described, and from the 1950s when the plasma factor was first named von Willebrand factor, up to 300 (<http://www.ragtimedesign.com/vwf/mutation/>) different mutations were founded throughout the 178 kb of DNA of the *VWF* gene.

It is not known if the extremely heterogeneity observed for VWD is based on the features of VWF as multifunctional protein, or on its complex biosynthesis with extensive post-translational processing and distinct pathways of intracellular transport and secretion. Faults could occur at any of this levels and could be associated with specific VWD types⁶⁰.

VWD was classified in three major categories⁶¹: type 1 is the most frequent (70-80 % of the cases), groups partial quantitative deficiencies (1-40% of normal VWF levels) and leads to highly variable phenotypes⁶²⁻⁶⁴, type 2 collect all qualitative deficiencies and type 3, the most rare (approximately 1/1 million), give rise to total deficiencies⁶⁵⁻⁶⁷.

Mutations related to decreased synthesis, impaired secretion, increased clearance or a combination of these conditions lead to low VWF plasma levels in type 1 patients. Several studies showed that in more severe VWD type 1 cases, genetic changes are common within the *VWF* gene and highly penetrant. Genetic determinants in milder VWD type 1 cases involve factors in- and outside the *VWF* gene^{68,69}.

Mutations causing type 2 VWD are often within *VWF* gene and interfere with protein structure or function⁶⁴. Type 2 is divided into 4 subclasses: type 2A, 2B, 2M and 2N.

2A is the most common qualitative abnormality of VWF and is associated with selective loss of large and intermediate-sized VWF multimers paralleled with decreased platelet-dependent function. The reduction of larger multimers is caused by either increased sensitivity to proteolysis by ADAMTS-13 or impaired multimer assembly within the Golgi^{70,71}.

2B is also characterized by loss of larger multimers. However, in VWD type 2B this is due to increased affinity of mutated VWF for the platelet GPIb-IX-V complex⁷². Gain-of-function mutations in the VWF-A1 domain lead to VWF with an abnormal conformation, which 'spontaneously' reacts with circulating platelets^{73,74}.

2M includes variants in which platelet adhesion is impaired, due to abrogated binding to GPIb α (i.e. the opposite of the VWD type 2B mutation). However, the VWF multimer distribution in these patients is normal⁷⁵.

Mutations in the *VWF* gene responsible for VWD type 2N cause defective binding to FVIII^{76,77}. In these patients FVIII is not stabilized by VWF and clinical symptoms are similar of those of Haemophilia A⁷⁸.

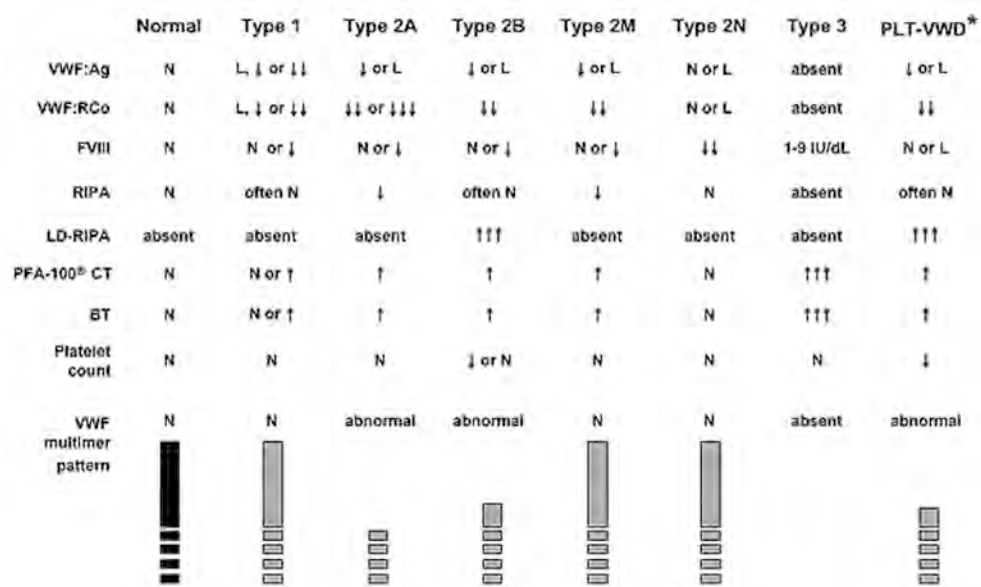


Figure 7: Schematic representation of expected laboratory values in VWD types (Montgomery RR http://www.nhlbi.nih.gov/guidelines/vwd/3_diagnosisandevaluation.htm)

In spite of great efforts to precisely describe and define single groups of mutations, many variations are controversially designated in different subtypes (Multiple pathophysiologic mechanism) for example the C1149R change⁶¹ and the "Vicenza" mutation⁵⁸ due to the complexity of the phenotype, and to discrepant interpretation of laboratory testing displaying an ample variation^{58,61}.

VWD TYPE 2A and subtypes IIC, IID and IIE/F

VWD 2A includes all patients displaying lack or decreased HMWMs paralleled with decreased platelet-dependent function. However the molecular mechanism resulting in the loss of HMWMs and the mode of inheritance could be different⁶¹.

VWD due to defective assembly of VWF structure can be produced by mutations in the propeptide, C-terminal “Cysteine Knot” or D3 regions.

In recessive type IIC VWD, homozygous or compound heterozygous mutations in the VWF propeptide preventing multimerization in the Golgi apparatus are associated with characteristic simple multimer pattern that is essentially devoid of satellite bands and pronounced first band. The propeptide has an essential role in promoting multimer formation, possibly by catalyzing disulfide interchanges resulting in the interdimeric disulfide bonds^{60,61,79}. The presence of CGLC sequence both in the D' and D2 domains (159-162 and 521-524 positions), which are homologous to the sequence of the catalytic site -CGXC- of the ER disulfide isomerase, support this notion. Mutations introduced at these positions result in unfeasible multimerization of recombinant VWF⁷⁹.

In type IID VWD, a multimer assembly defect is associated with heterozygous mutations in the CK domain preventing dimerization in the ER. As a result both proVWF monomers and wild type dimers arrive in the Golgi where the binding of a mutated monomer to a normal dimer terminates the polymerization process at that extremity. The multimer pattern shows, in addition to normal multimer bands, less intense and odd intervening sub-bands located between normal oligomers containing small multimers made by normal dimers and mutated monomers^{60,61,79}.

In type IIE/F VWD, the cause of the multimerization inefficiency, have to be found in heterozygous mutations located within the D3 domain, often affecting Cys residues and interfering with inter-subunit disulfide bond formation in the Golgi during dimers association to form multimers. The resultant multimer pattern is often “smeary” that suggests an heterogeneous disulfide bond structure. Some other mutations in the D3 domain are not associated to aberrant disulfide bond formation and result in different phenotype (i.e. type 2M “Vicenza VWD”) ^{60,61,79}.

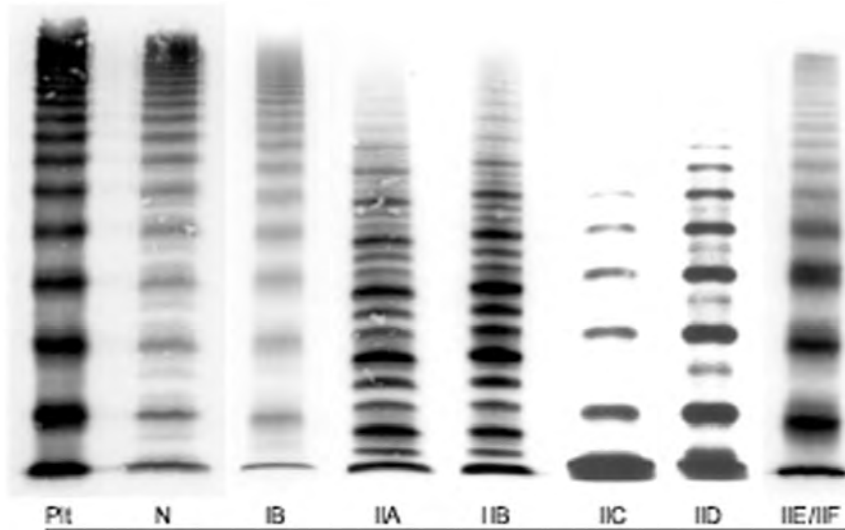


Figure 8: Multimer analysis of VWF from the plasma of patients with different VWD types compared with normal control reported by Schneppenheim R et al.⁶⁰ (gel concentration 1.5%). Plt = platelets's VWF, displaying the characteristic presence of 'supranormal' multimers and the lack of a triplet structure. Normal multimer pattern (N) displays a typical triplet structure and the high molecular weight multimers appear pronounced. Type IIC is associated to the lack of HMWMs and absence of a triplet structure of individual multimers. LMWMs and especially the first band, are markedly pronounced. Intervening bands as in VWD IID, representing multimers with an odd number of monomers, are absent. The similarity between types IID and IIC is based on the absence of a triplet structure, the lack of high molecular weight multimers, and the pronounced bands of smaller multimers, albeit not as marked as in type IIC. The intervening bands result from the dimerization defect. The type IIE/F multimer pattern is characterized by a lack or relative decrease of HMWMs and the absence of the outer sub-bands of the normal triplet structure. Inner sub-bands, closer to the central band, are present, which give the individual multimer a broader appearance⁶⁰.

RNA-INTERFERENCE: CORRECTION APPROACH TO DOMINANT DISEASES

RNA interference (RNAi) is a recently discovered mechanism in which gene expression is regulated by small double-stranded RNA (dsRNA) molecules that inhibit gene expression with complementary nucleotide sequences⁸⁰. The RNAi machinery acts by either suppressing transcription (transcriptional gene silencing) or activating a sequence-specific RNA degradation process (post-transcriptional gene silencing)⁸¹.

Essentially RNAi (Figure 9) is divided in two major steps. First, in the "RNAi-initiating step" large dsRNA are bound by RNA nucleases and cleaved in discrete 21- to 25-nucleotide RNA fragments called small dsRNAs. In the second step, these short dsRNA molecules (called miRNAs if derived from endogenously cleaved long dsRNA, or siRNAs if exogenously synthesized and introduced inside cells) are associated in the cytoplasm with a protein complex defined as RISC (RNA-induced silencing complex), one of the two RNA strand is degraded and the remaining guide strand mediates the sequence-specific degradation of the corresponding mRNA (in the case of siRNAs) and/or translational repression by binding to the 3' untranslated region (UTR) in the case of miRNAs⁸⁰⁻⁸².

The existence of the RNAi machinery, that mediate gene expression regulation and/or, in some cases, protection from dangerous (i.e. viral) external RNAs, also give the opportunity to take advantage on this endogenous process to induce the silencing of virtually any gene of interest⁸⁰.

For this reason RNAi-mediated silencing is recently become an extremely used and useful tool in the reverse genetic analysis of gene functions and it also represents a potential novel drugs for the treatment of diseases⁸⁰.

Due to the apparent simplicity of the mechanism, which offer almost unlimited silencing applications based only on the sequence availability of the mRNA you want to silence, a large and increasing number of studies have reported fascinating application of the RNAi strategy to numerous disease for which effective treatment are currently unavailable or sub-potential, i.e. viral infection, cancer, autoimmune- neurodegenerative- and cardiovascular-diseases,... although some important and not omissible limitations have not yet been resolved⁸⁰.

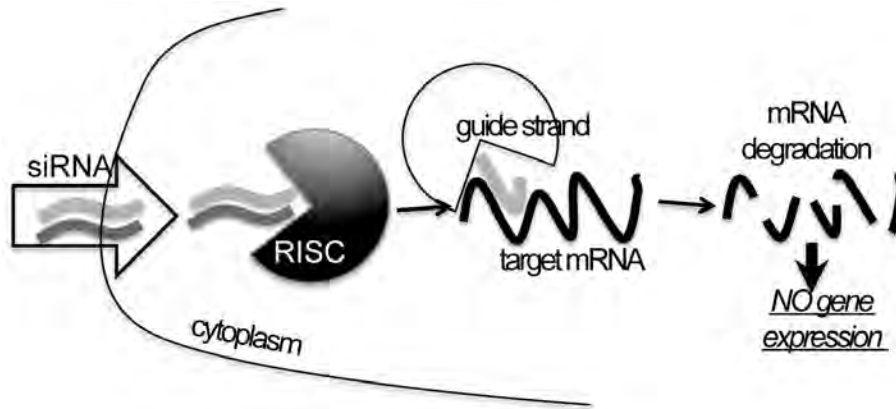


Figure 9: Simple schematic representation of the RNAi mechanism focusing on the exogenous siRNAs silencing action.

The major impediment for the clinical use of siRNAs is their poor cellular uptake and short serum half-life. Although great progress has been made on this regard, researches are currently open to find the most selectively, safe and potent delivery system for siRNAs.

In spite of this, numerous preclinical studies allowed the establishment of some clinical trials: phase I-II for age-related macular degeneration (AMD) and respiratory syncytial virus (RSV)⁸⁰.

The primary aim of human gene therapy is to correct the genetic disorder caused by mutation specific effects. Basically recessive disorders are approached with replacement therapy that, introducing wild type allele, restores gene function and improves disease pathology. On the other hand dominant phenotypes may be caused by haploinsufficiency (reduction of the wild type protein level), by gain of function mutation or both. The suppression of the detrimental effects of the mutated allele together with the maintenance of the wild type allele expression are necessary to overcome the effects of a gain of function mutation. These features make dominant inherited diseases perfect candidates for RNAi-based gene therapy⁸³.

Several dominant disorders have already been approached, *in vitro* or in animal models, with RNAi such as Huntington's disease (HD), spinocerebellar ataxia type 1 (SCA1), amyotrophic lateral sclerosis (ALS),

Alzheimer's disease, myotonic dystrophy (DMI) all caused by triplet expansion.

When dominant mutations occur within gene coding for protein which needs to aggregate to function properly, a dominant-negative effect is expected. In this case a severe phenotype is often observed, because wild type and mutant proteins interact and also the wild type molecule is not available to carry out its function.

Mutations with dominant-negative effect are classically detectable in structural proteins i.e. collagen or nonstructural proteins that dimerize or oligomerize i.e. transcription factors of the b-HLH-Zip family, which bind the DNA as dimers, or ion channels located in cell membranes, which are often multi-protein complex⁸⁴.

Recently are reported that RNAi-mediated gene silencing could be a promising treatment for the pachyonychia congenita^{85,86} (PC), which represent one of the numerous skin disorder associated to one of the 54 human keratin genes, and is associated to dominant-negative mutations. PC represent a suitable disease to test RNAi treatment because offer some advantages such as the presence of recurrent mutations, and the external location and focal nature of the plantar skin lesions permitting minimally invasive localized treatments to be performed on patients. The discover of potent and selective siRNA targeting the most common mutation causing PC resulted in the initiation in 2008 of a clinical trial for this skin disorder.

VWF displays extraordinary adhesive features: it polymerizes with itself and exploits its function through the binding with collagen, platelet receptors and other ligands. For these reasons it is expected that mutations in the related *VWF* gene could have dominant-negative effect. Furthermore VWF is synthesized in endothelial cells and megacaryocyte only, suggesting that, in the future, the treatment could be localized to these cell types.

Finally VWD is the most prevalent hemostatic disorder and the majority of its cases are dominantly inherited and could be potentially approached with RNAi treatment.

However, on the contrary to PC, over 300 mutations are associated to VWD and none of these is demonstrated to be the most prevalent. This would imply that very specific siRNAs have to be designed and tested for each VWD-associated mutations that you want to correct.

VWF is also a large protein that undergoes numerous and regulated post-transcriptional modifications and the setting studies to found effective siRNAs molecules need to be careful and rigorous.

For the sake of clarity some important advises for RNAi study design are reported below^{81,83}.

The use of siRNAs to silence gene expression in mammalian cells involves a careful consideration of selecting the siRNA sequences in the target gene to avoid non specific complementarity to unrelated genes and to avoid the choice of target site not accessible for the binding of the siRNA. It may be necessary to screen several sequences, concentrations, combinations and delivery systems to identify the most efficacy molecule for each cellular model. Today are available helpful on-line software, that provided RNA structure models to give information on the site accessibility or offering automated researches for siRNAs sequences with more probability to be effective that can help in the choice of siRNAs molecules. In addition it is essential to accurately optimize the transfection protocol depending on: the target cell type, the selected means such as siRNAs or vector-driven shRNAs and the delivery system.

BACKGROUND INFORMATION OF THE
p.P1105_C1926delinsR GENE DELETION AND OUTLINE
OF THIS THESIS

We have previously described a large, *de novo* and heterozygous deletion in *VWF* gene associated to a variant type 2 VWD. The proband showed a severe VWF deficiency, as indicated by reduced ristocetin cofactor activity (3%) and prolonged bleeding time (20 minutes), which produced a number of bleeding symptoms requiring blood transfusion⁸⁷. The altered multimer pattern (Figure 10) was characterized by reduced intermediate- and no HMWMs in plasma and platelets, and by abnormal morphology of triplets with a broad band apparently containing a fast-migrating component. Antigen (VWF:Ag) levels (24%) and FVIII coagulant activity (29%) were also reduced⁸⁷. The gene deletion boundaries were mapped within introns 25 and 34⁸⁸ and the new junction between exons 25 and 35 was sequenced after reverse transcription of the platelet RNA (Figure 11). At the protein level Cysteine 1104 should be connected in-frame with mutated codon 1926 (cysteine to arginine).

The encoded protein (Figure 12) would lack the last part of the D3 domain, the A1, A2 and A3 modules, and the first part of the D4 domain, which would virtually abolish, in addition to the A domain-associated adhesive function⁸⁹⁻⁹², the D3 domain-associated inter-dimer disulfide bond formation^{93,94} and thus multimerization. However, the dominant-negative attitude of the deleted protein still needs to be demonstrated, and its molecular features dissected. Dimerization and multimerization, distinct property of VWF producing extremely large and adhesive molecules, provide the rationale for the dominant inheritance caused by the interaction of wild type and mutant VWF monomers during polymerization. The strength of the negative effects produced by dominant variants would be associated with the ample variation of residual VWF level and function, and would participate in the phenotypic penetrance and severity of VWD types inherited as dominant traits, which is rather high⁹⁵. These are major open questions in VWF biology and VWD molecular bases definition.

In this study we constructed a cellular model of this unique disease variant as a tool to demonstrate the presence, and evaluate the efficiency, of the dominant-negative effect of the deleted protein in the biosynthetic steps of VWF maturation and secretion. This cellular model mimics patient's plasma VWF phenotype and highlights the key role of heterodimer between normal and deleted VWF molecules. We also propose a silencing approach to correct the dominant-negative effect that partially restored VWF levels.

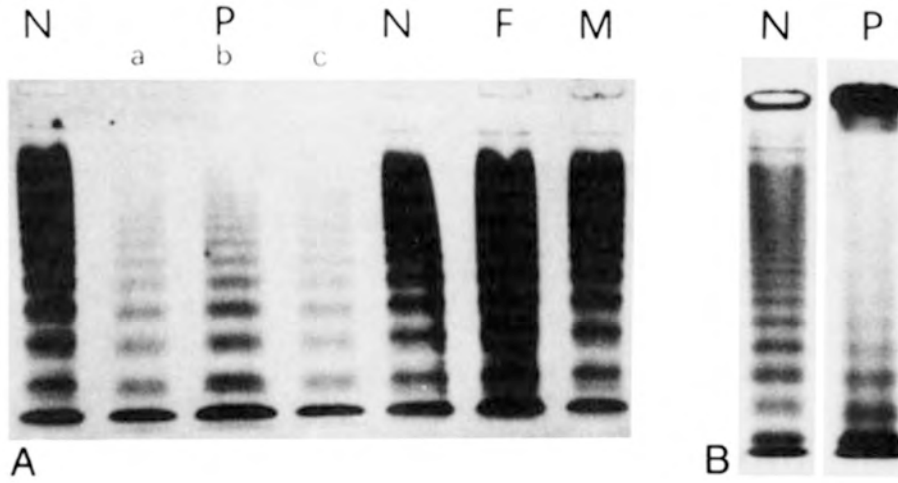


Figure 10: Multimer analysis of plasma (A) and platelet (B) and densitometric scans (C) reported by Bernardi F et al.⁸⁷ N: normal control; F and M. father and mother of the propositus (P). In lane b a double amount of plasma of the propositus was loaded and in lane c an antiproteolytic mixture was added as anticoagulant. (C) Densitometric analysis of lanes reported in (B).

	N	P	F	M	B
bleeding time (min)	5-8	20	5	7	8
FVIII:C	60-170	29	98	70	75
VWF:Ag	60-150	24	98	102	72
Ri:Cof	60-150	3	93	76	70

Table 1⁸⁷: Hemostatic parameters in members of the propositus's family as in Bernardi et al. 1990 Blood. N = normal range, P = propositus, F = father, M = mother, B = brother.

Background Information of the p.P1105_C1926delinsR

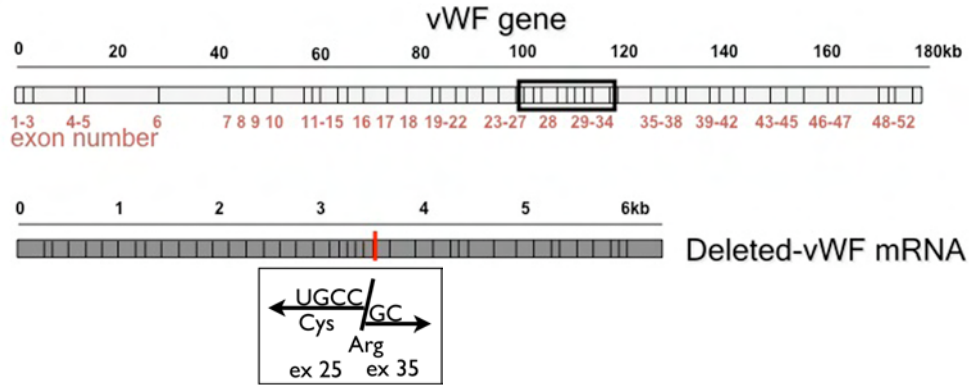


Figure 11: Schematic representation of the deletion location within VWF gene and the resultant deleted mRNA. The box indicates the new junction that connected in-frame exons 25 and 35 thus mutating Cys 1926 to Arg.

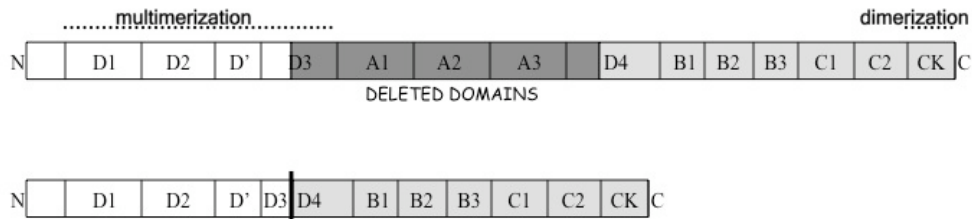


Figure 12: Schematic representation of the wild type and deleted VWF protein domains. Dark-grey motifs (1105-1925 amino acids) are missed in the deleted VWF.

MATERIAL & METHODS

Creation of expression vectors

The expression vector pSVHVWF1 for human VWF, having the full-length VWF cDNA cloned into the pSV7d plasmid, was a generous gift from Prof. J.E. Sadler (Washington University in St. Louis)²⁵.

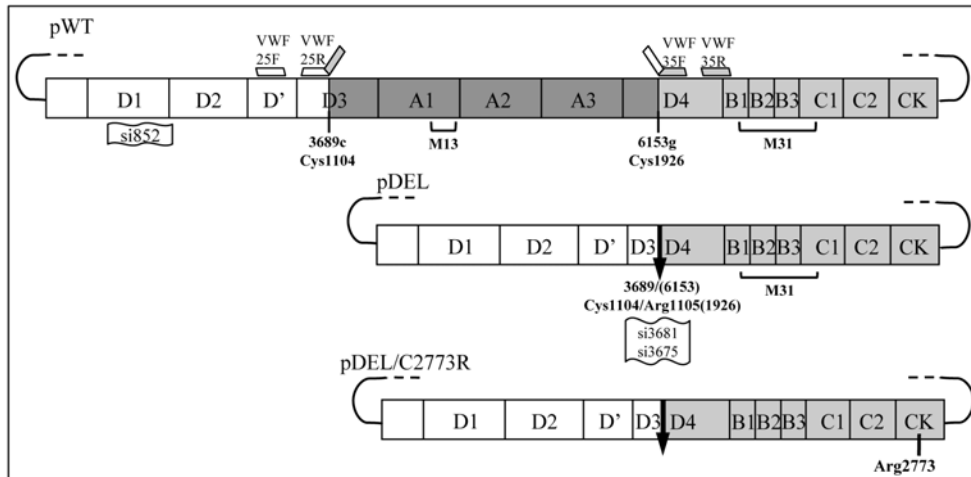


Figure 13: Schematic representation of wild type, deleted and double mutated VWF-expression vectors. Black arrow within pDEL and pDEL/C2773R indicates the breakpoint. Black bordered flags indicate siRNAs complementary regions. Squared brackets indicate epitopes recognized by antibodies utilized in Western blotting experiments.

To create the pSVHVWF-P1105_C1926delinsR^{96,97} (Figure 13) deleted expression vector (defined as pDEL) the *SacI* restriction site at position 8876 was initially abolished by site-directed mutagenesis through the mutagenic primers 5'CCACAATAAAGGCTCAGCTCTTATCTTGC^{3'} (change underlined) and 5'GCAAGATAAGAGCTGAGCCTTTATTGTGG^{3'} by using the QuikChange XL Site-Directed Mutagenesis Kit (Stratagene, La Jolla, CA). The transient expression of the pSVHVWF variant in monkey kidney cells (COS-1) resulted in secreted VWF antigen and VWF collagen-binding activity levels indistinguishable from that of the pSVHVWF1, and pSVHVWF was subsequently used as wild type VWF expression vector (pWT).

To reproduce the P1105_C1926delinsR deletion we exploited the overlapping PCR strategy^{98,99} (Figure 14) with appropriately designed

primers. Primers 5'CAATGACCTCACCAGCAGCAACC3' (VWF-25F) and 5'TGCCTGTGCACACGCGGCACAATGTGGCCGTCCTCC3' (VWF-25R), having a 15 bp-tail complementary to nt 6153-6167 in exon 35, were used to amplify the region upstream of the breakpoint. Primers 5'CGGCCACATTGTGCCGCGTGTGCACAGGCAGCTCC3' (VWF-35F), having a 15 bp-tail complementary to nt 3675-3689 in exon 25, and 5'TCTTCAGGGACACAGCTGCC3' (VWF-35R) were used to amplify the region downstream of the breakpoint. The partially overlapping regions were amplified using the pWT as template (30 cycles; 30" at 94°C, 30" at 55°C, 50" at 72°C). Amplicons were then purified and mixed for a third PCR reaction using the VWF-25F and VWF-35R external primers. (30 cycles; 30" at 94°C, 30" at 50°C, 1' at 72°C). The resulting 1279 bp fragment was then cloned into the pWT vector utilizing SacI restriction sites at positions 3395 and 6986.

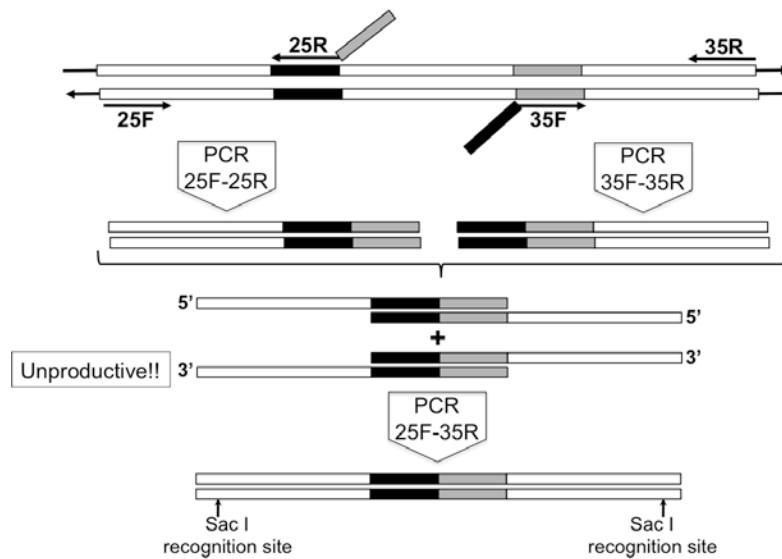


Figure 14: Schematic representation of the overlapping strategy applied to produce the deleted vector.

To create the pDEL/C2773R (Figure 13) vector the C2773R mutation was inserted into the pDEL vector by site-directed mutagenesis using primers 5'GAGACGCTCCAGGACGGCTGTGATACTC3' and 5'GAGTATCACAGCCGTCCTGGAGCGTCTC3'.

The correct sequence of vectors, and the absence of undesired changes, was confirmed by direct sequencing.

Expression of recombinant VWF in eukaryotic cells

COS-1 cells were used for transient expression of VWF variants²⁵. Cells were grown in Dulbecco modified Eagle's medium (D-MEM) supplemented with 2 mM L-glutamine, 50 IU/ml penicillin, 50 µg/ml streptomycin, and 10% (vol/vol) fetal bovine serum and seeded at 60-70% confluence into 6-well plate for transfection. Single plasmids, or combination of them in the relative molar proportion reported in the figures were transfected into COS-1 cells by using Lipofectamine2000 (Invitrogen, Carlsbad, CA) and in the presence of Opti-MEM serum-free medium (Invitrogen). The total amount of DNA in each transfection was set to 4.5 µg by adding, when needed, a gutted pUC18 plasmid. Seventy-two hours after transfection the conditioned media were collected and cells were lysed for total RNA isolation (NucleoSpin RNAII isolation Kit, Macherey-Nagel GmbH&Co. KG, Duren, Germany) or intracellular VWF investigations (lysis buffer: NaCl 150 mM, Triton X-100 1%, Tris HCl pH 7.4 50 mM, PMSF 1 mM, Benzamidine 10 mM).

Silencing

The siRNA 852 (sense, 5'CCUCGGACCCUUAUGACUUUU^{3'}; antisense 5'AAGUCAUAAGGGUCCGAGGUU^{3'}), to specifically silence the wild type VWF expression, and the siNC (sense, 5'CCUCAGUCCUAUAGCGCUUUU^{3'}; antisense 5'AAGCGCUAUAGGACUGAGGUU^{3'}), as negative control, were designed by the Invitrogen software BLOCK-iTTM RNAi Designer (<https://rnaidesigner.classic.invitrogen.com>) and purchased (Figures 13-14).

Conversely, none of the on-line available software programs for the siRNA design were able to predict a siRNAs targeting the naturally occurring breakpoint region of the mutated VWF variant, and hence able to selectively inhibit the pDEL expression.

To overcome this limitation we first evaluated the VWF mRNA conformation at the breakpoint region and its theoretical accessibility to complementary siRNA with the Mfold¹⁰⁰ software (<http://mfold.bioinfo.rpi.edu/>).

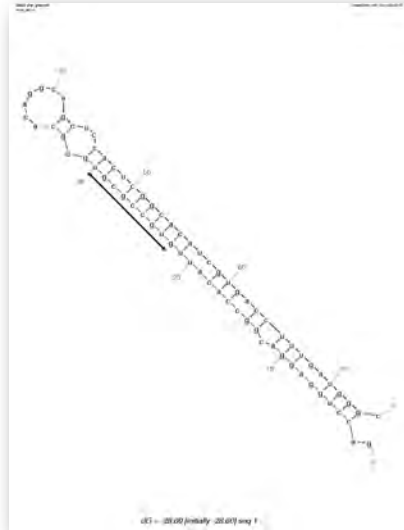


Figure 15: Example of RNA fold made by the mfold on-line software. The figure showed a small part of the entire RNA structure of the deleted molecule surrounding the breakpoint (bold line). In this simplified image the availability of the site is evident.

The si3681 (sense 5'CAUUGUGCCGCGUGUGCACUU^{3'}; antisense 5'GUGCACACGCGGCACAAUG UU^{3'}) and the si3675 (sense, 5'CGGCCACAUUGUGCCGCGUUU^{3'}; antisense, 5'ACGCGGCACA AUGUGGCCGUU^{3'}) oligoribonucleotides complementary to the breakpoint region were then designed (Figure 16-17) in the respect of the siRNA design rules and purchased from Invitrogen.

siRNAs (10-80 nM) were transfected, with VWF expression vectors in COS-1 cells by Lipofectamine2000 (Invitrogen). Medium was replaced with fresh Opti-MEM 4 hours after transfection. Conditioned media and cells were collected as above mentioned.

Preliminary studies were conducted to achieve the most efficacy silencing activity of the si3675 and si3681 and their combination toward the pDEL expression, and the appropriate experimental conditions to avoid adverse effects. Treatment with 40 nM of si3681, complementary to the breakpoint sequence exactly in the middle of its sequence, was chosen as the most efficient.

Material and Methods

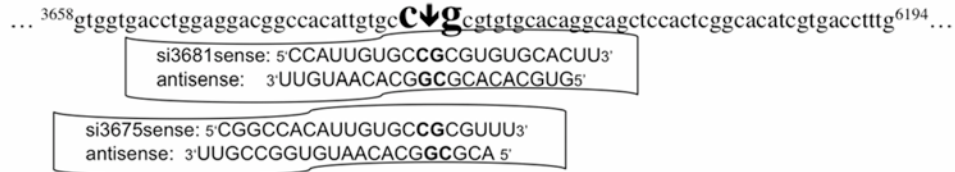


Figure 16. Deleted VWF sequence fragment and siRNAs. Position and sequence of the mRNA and of the siRNAs (flags) directed to the mRNA breakpoint (3' of exon 25 and 5' of exon 35). Nucleotides at the junction (arrow) are indicated by bigger/bold letters.

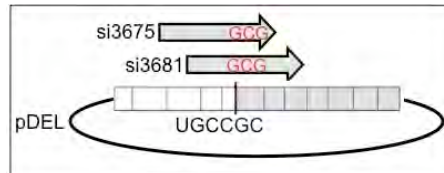


Figure 17: Schematic representation of siRNAs targeting region (across the breakpoint) within pDEL.

mRNA study

Reverse-transcription (RT) was performed using “SuperScript III First-Strand Synthesis System” (Invitrogen) and oligo (dT). PCR amplification (30 cycles; 30” at 94°C, 30” at 50°C, 30” at 72°C) was performed with forward primer 5’CAGTGACGTCTTCCAGGAC3’ and reverse primers 5’AGGGTCACTGGGATTCAAGG3’ and 5’TGCCTGTGCACACGCGGC3’ designed on pWT and pDEL vectors, respectively. Capillary electrophoresis was performed on the Experion automated electrophoresis station¹⁰¹ (Bio-Rad Laboratories, Hercules CA, USA) to detect amplification products. This method applies a combination of microfluidic separation technology and sensitive fluorescent sample detection to perform, in our cases, RNA automated analysis. All gel-based electrophoretic steps are automatically performed to generate reproducible separation and quantitative results, which may be reported as an electropherogram gel image (Figure 31A) or scheduled.

Antibodies

Polyclonal Rabbit anti-human VWF (A0082), polyclonal rabbit anti-human VWF/HRP (P0226), polyclonal swine anti-rabbit immunoglobulins/TRITC (R0156) and polyclonal Goat Anti-Mouse IgG/HRP antibodies were purchased from DAKO (DAKO, Glostrup, Denmark). The mouse monoclonal [2G11] antibody to Mannose 6-Phosphate Receptor (late endosomes marker) (ab2733) and the mouse monoclonal [1D3] to PDI (ER marker) (ab12225) were purchased from Abcam (Cambridge, UK). The FITC-conjugated AffiniPure goat anti-mouse IgG (H+L) (115-095-146) was from Jackson ImmunoResearch Laboratories (Baltimore, USA). Monoclonal anti-VWF M31 and M13 were obtained as described^{102,103}.

Analysis of recombinant VWF

VWF:Ag in conditioned media and cell lysates was determined by an ELISA assay performed with above mentioned Dako antibodies (Polyclonal Rabbit anti-human VWF and polyclonal rabbit anti-human VWF/HRP). The ELISA assay described by Federici et al.¹⁰⁴ was tested and partially modified to obtain better results. Essentially the blocking solution is based on PBS instead of TBS because, although both showed good response to scalar dilutions of a pool of normal plasma, the first one showed lower values of background. In order to increase the relative absorbance of each samples several primary antibody concentrations are tested but all of these gave similar good results. When different concentrations of secondary antibody are used a good improvement in the absorbance values was obtained doubling (1 µg/ml) the proposed concentration (0.5 µg/ml). Intra-assay coefficient of variation was ≈ 6.5% and the inter-assay was ≈ 15%. Sensitivity was ≈ 2 ng/ml.

VWF:CB was measured in conditioned media using the “CollagenBinding Assay kit” (Life therapeutics, Clarkston, USA).

Multimer analysis: the multimeric structure of VWF was detected in sodium dodecyl sulfate (0.1%) agarose gel (1.5-3%) electrophoresis^{105,106} followed by Western blotting and detection with immunoenzymatic stain (polyclonal Goat Anti-Mouse IgG/HRP antibodies, Dako) or with radioactive detection (¹²⁵I-anti-vWF antibody¹⁰³).

Western blotting of VWF present in media and lysates were performed in polyacrylamide gel (NuPAGE4-12% Bis-Tris Gel, Invitrogen) in reducing condition. The electrophoresis was performed in MOPS 1x buffer (Invitrogen) for approximately 5 hours at 200 V, followed by transfer in TRIS (25 mM)-glycine (192 mM) buffer with methanol (10% v/v) and sodium dodecyl sulfate (0.7 mM) at 300 mA for 2 hours. The nitrocellulose membranes were reacted with different anti-VWF monoclonal antibodies followed by incubation with anti-mouse Immunoglobulins/HRP (Dako). Bands were visualized by autoradiography with Amersham Hyperfilm ECL (GE Healthcare Limited, Pollards Wood, UK) using “Super Signal West FEMTO Maximum Sensitivity Substrate” for media and “Pierce ECL Western Blotting Substrate” for lysates (Pierce, Rockford, USA).

Immunofluorescence microscopy

Cells for immunofluorescence labelling were cultured at sub-confluence in 6- or 12-wells on a coverslip of 12 or 24 mm of diameter. Cells were transfected with Lipofectamine2000 lipid reagent (Invitrogen) using a 2:1 ratio for Lipofectamin/vectors. 24 hours after transfection cells were fixed in methanol for 7 minutes at -20°C and saturated with 4% Bovine Serum Albumin (BSA)/PBS. Subsequent incubation with primary and appropriate secondary antibodies was performed for 1 hour at room temperature. Primary antibodies were diluted 1:100 in 4% BSA/PBS and secondary antibodies were diluted 1:50 in the same solution.

Images were acquired with a Nikon fluorescence microscope Eclipse 50i (Nikon Instruments, Sesto F.no, Firenze, Italy) equipped with DS-5M digital camera and DS-L1 control unit. Objectives used were Nikon Plan 20x/0.5 and 40x/0.75 and Nikon 100x/0.5-1.25 Oil Iris.

Confocal images were acquired as previously described¹⁰⁷ with a Zeiss LSM 510 microscope equipped with a Fluar 40x/1.3 oil immersion objective (Carl Zeiss, Arese, Italy). Briefly, 488 and 543 nm excitation wavelengths were provided respectively by Agron/2 and HeNE laser sources at a 5% intensity.

Superimposition of red and green fluorescence, not specifically due to co-localization, was excluded by applying to the green channel a beam path admitting the acquisition of fluorescence comprised among 505 and 550

Material and Methods

nm and to the red channel a light path excluding all fluorescence below 560 nm. Pinhole values were ranging from 40 to 80 μm . Where required, image magnification was obtained digitally with the LSM examiner software (Carl Zeiss).

RESULTS

Creation of the recombinant deleted expression vector (pDEL)

To create the deleted expression vector pSVHVWF-P1105_C1926delinsR^{96,97} (pDEL), the overlapping PCR method was used. First we identified a fragment of the pSVHVWF1 vector containing the region to be deleted and delimited by SacI restriction sites. Downstream of the deletion, near the end of the VWF cDNA in the pSVHVWF1 vector, a third Sac I recognition site was present thus complicating the subsequent cloning step. To overcome this limitation we abolished the last Sac I (position 8876) restriction site through site-directed mutagenesis and produced the pSVHVWF (pWT) expression vector. The transient expression of the pSVHVWF variant in COS-1 cells resulted in secreted VWF antigen and collagen-binding activity levels indistinguishable from that of the pSVHVWF1, and pSVHVWF was subsequently used as wild type VWF expression vector (pWT) (Figure 18).

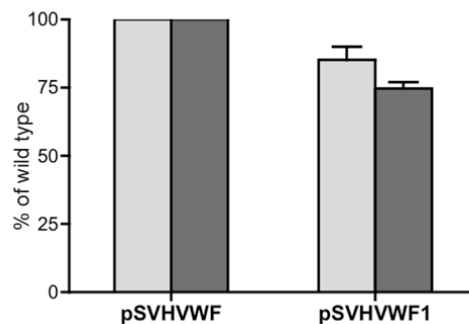


*Figure 18: VWF:Ag (light grey) and VWF:CB (dark grey) levels in conditioned media from cells transiently transfected with pSVHVWF or pSVHVWF1. Mean values of three replicate of pSVHVWF were used as 100% (570.6 ng/ml for antigen value and 152.3% of normal standard as CB value) and the mean of three replicate (\pm SEM) was used to evaluate pSVHVWF1 levels. *t* test was applied to exclude significative differences.*

The overlapping PCR^{98,99} was performed on this mutagenized vector. First two separate PCR reaction were performed with primers 25F-25R and 35F-35R, the pWT vector was used as template (Material & Methods Figure 14 and Figure 19).

Results

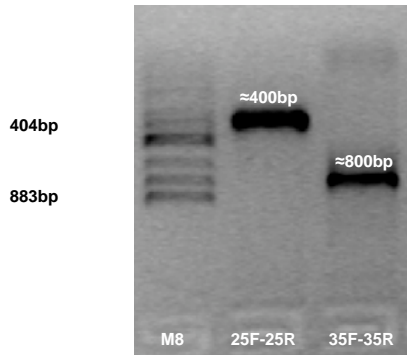


Figure 19: Electrophoretic separation of partially overlapping fragments amplified in the two separate PCR step performed with 25F-25R and 35F-35R set of primers.

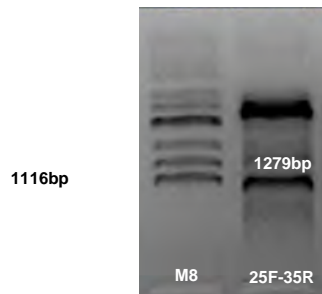


Figure 20: Electrophoretic separation of the 1279 bp fragment that connected residues 3689 and 6153 thus “containing the deletion.”

The amplicons obtained, which partially overlap (Material and Methods, Figure 14) were electrophoresed on agarose gels, excised, purified and used as template for the third PCR amplification reaction performed with external 25F and 35R primers (Figure 20).

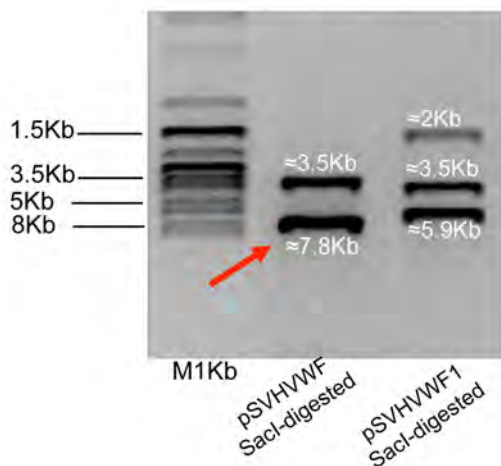


Figure 21: Electrophoretic separation of pSVHVWF and pSVHVWF1 expression vectors digested with Sac I restriction enzyme. The arrow indicate the fragment excised and purified for the subsequent ligation step.

The 1279 bp fragment carrying the desired junction between nucleotides 3689 and 6153, contained two Sac I recognition sites at each extremity and was then digested with Sac I restriction enzyme. Accordingly, the pWT vector that contained two recognition site, at positions 3391 before the breakpoint, and at position 6892 downstream of the breakpoint, was digested with the Sac I enzyme to produce compatible ends with the above described fragment containing the desired junction (Figure 21).

Finally the ligation between the “7.8 Kb fragment” and the digested “1279 bp” fragment was performed.

The resulting pDEL expression vector, which would produce a protein containing the expected junction between exons 25 and 35, was used to transfect COS cells alone or in combination with pWT vector.

Expression of the in-frame deleted VWF

In order to investigate the molecular mechanism through which the heterozygous deletion P1105_C1926delinsR produced the severe VWD phenotype we first studied the expression of the deleted VWF both in media and cell lysates in the absence of the wild type protein (Figure 22).

For this purpose two antibody pools^{102,103} were used in Western blot analysis. The M31 pool (Figure 22A, left panels) reacts with VWF residues 2244-2456, downstream of the breakpoint (Material and Methods, Figure 13), and would recognize only domains with a normal reading frame. The M13 pool (Figure 22A, right panels) reacts with VWF residues 1394-1473, located within the deletion boundaries and thus only with the wild type VWF. The comparison of blots supported that the pDEL vector efficiently drove the biosynthesis of the in-frame deleted molecule. The deleted VWF appeared to be only partially secreted (Figure 23), and its electrophoretic migration was compatible with the protein size (\approx 160 kDa) inferred from the extent of the deleted domains (821 amino acids).

Whereas traces of the altered pro-VWF were detectable in lysates, only the mature form of the deleted VWF was secreted. Pro-wild type VWF was abundant both in media and lysates, in accordance with published data^{25,29,30}. Antigen and collagen-binding levels in media from cells expressing the pDEL vector (Figure 22B) were very low and undetectable, respectively. The multimer analysis in high resolution gels (Figure 25 -page 40) showed the presence of a broad band with increased mobility as compared to wild type, and did not reveal the presence of tetramers.

Results

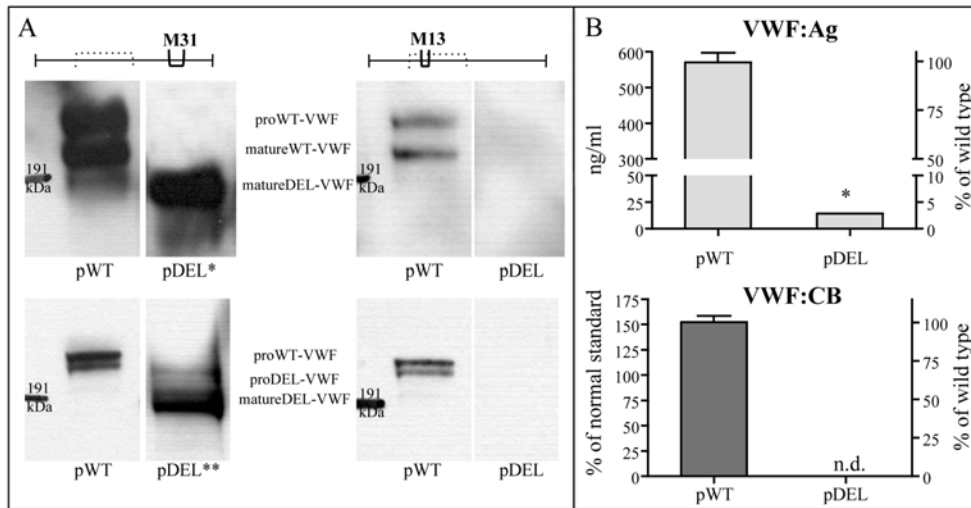


Figure 22. Expression of the deleted VWF.

(A) Western blot analysis of wild type and deleted VWF performed on conditioned media (upper panels) and cell lysates (lower panels) with monoclonal antibody pool M31 and M13^{102,103}. The M13 antibodies, targeting VWF A1 domains (right panels), recognize only wild type VWF. The M31 antibodies (left panels), targeting the C-terminal domains, indicate the in-frame translation of the deleted VWF. Migration of the mature wild type (matureWT-VWF) and deleted (matureDEL-VWF) proteins, and of forms containing the propeptide (proWT-VWF and proDEL-VWF), are indicated. In cell lysates additional bands containing the pro-wild type VWF and the pro-deleted VWF are detectable. The asterisks indicate (*) over-exposure or (**) under-exposure of gels. (B) VWF:Ag (upper panel) and VWF:CB (lower panel) levels in conditioned media of COS-1 cells. Results (ng/ml) of three independent experiments are reported as Mean \pm SEM. The right y axis indicates the percentage of wild type (100% VWF:Ag, 570.6 ng/ml; 100% VWF:CB, 152.3 of normal standard). Statistical significance (* $P < 0.001$) was evaluated by one-way ANOVA with Bonferroni post-test. n.d., not detectable.

Results

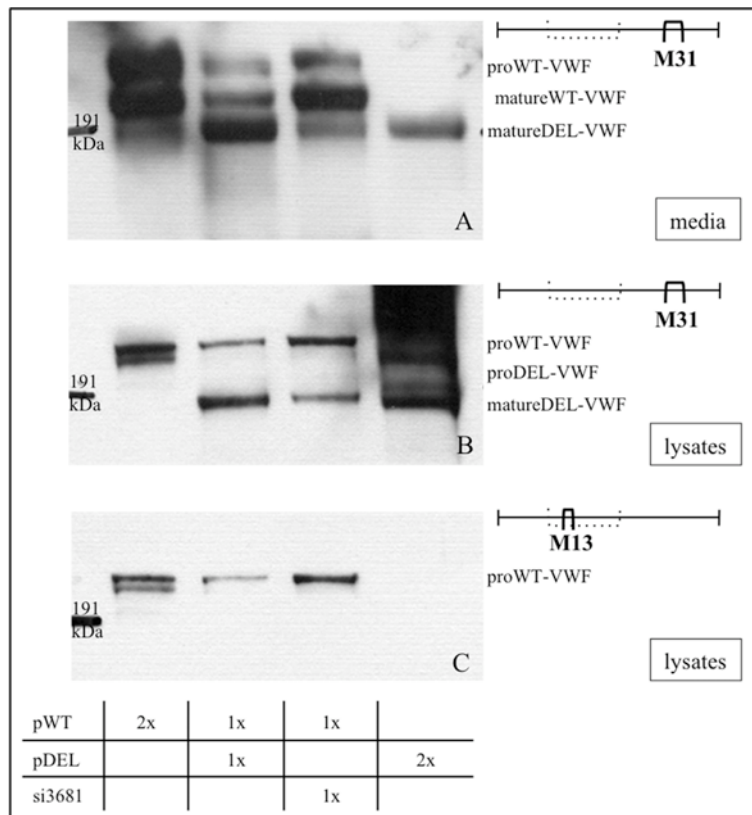


Figure 23: Intact Western blot containing the entire panels displayed in Figure 22, Figure 24 and Figure 31. The relative molar amounts of vectors and siRNA are indicated in the table. Antibodies are indicated as in figure 22. Conditioned media (panel A) were tested by the monoclonal antibody pool M31. Cell lysates (panels B and C) were tested by monoclonal antibodies M31 and M13.

Dominant-negative effect of the VWF deletion – cellular model

To mimic the heterozygous condition in COS-1 cells, the pWT vector was co-expressed with increasing amounts of the pDEL, which progressively decreased the levels of wild type VWF (Figure 24). Equimolar amounts of both plasmids produced 20% (112.3 ± 4.1 ng/ml, Figure 24A, upper panel) of wild type antigen levels (570.6 ± 26.5 ng/ml), and 2% of collagen-binding activity (Figure 24A, lower panel). Accordingly, the ratio between VWF:CB and the antigen values dropped to 1/10 of that calculated for the wild type. A double proportion of the deleted vector decreased the VWF:Ag levels to

12% (70.6 ± 4.5 ng/ml) of wild type, and abolished the collagen-binding activity.

The Western blotting, performed in reduced conditions (Figure 24B) and thus able to evaluate the proportion of the normal and deleted VWF molecules, indicated that in co-expression experiments the altered VWF prevailed. Taking into account the pro-peptide and mature forms, the densitometric analysis in media and lysates indicates that the ratios between the altered and normal VWF were 1.8 and 3.5, respectively. Moreover, the absolute amounts of the deleted protein appeared to be increased in media from cells expressing both vectors (Figure 23).

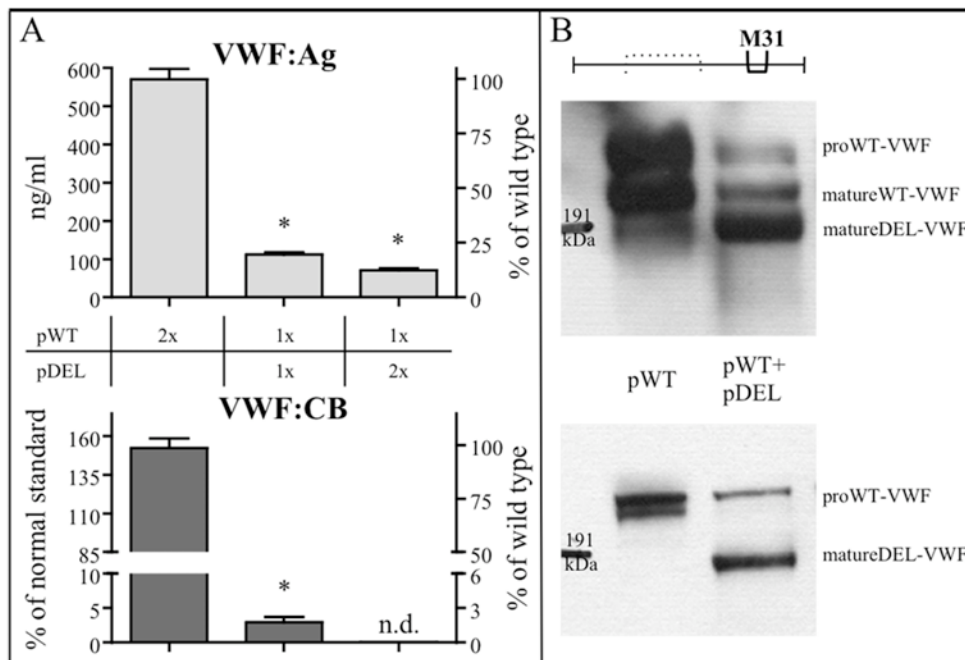
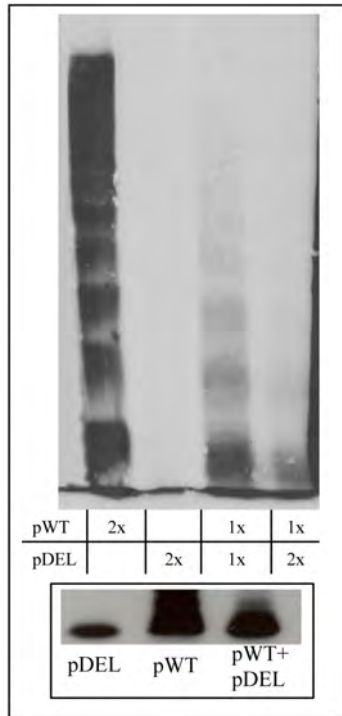


Figure 24. Dominant-negative effect of the in-frame deleted VWF variant. (A) VWF:Ag (upper panel) and VWF:CB (lower panel) levels in conditioned media of COS-1 cells. The relative molar amount of pWT and pDEL vectors is reported in the table. The right y axis and statistical analysis as in Figure 22. (B) Western blot experiments in conditioned media (upper panel) and cell lysates (lower panel) with antibody pool M31.

Results



(C) Multimer pattern detected with immunoenzymatic stain from media obtained as described in the table. The inset reports samples tested by ^{125}I -labelled-anti-vWF antibody to better visualize the deleted VWF form.

The multimer analysis (Figure 24C and 25) of VWF in media from co-transfected cells indicated that the pDEL expression impaired secretion of oligomers, particularly the HMW forms, in a dose dependent manner. A detailed interpretation of the observed pattern is complicated by the similar extent of the deleted (821 amino acids) and propeptide region (741 amino acids), which causes co-migration of dimers (D) and tetramers (T) with different subunit composition (i.e. homodimers D_A and heterodimers D_C , Figure 26). In spite of this limitation, the presence of heterodimers (D_B) between the wild type and deleted proteins was clearly detectable. As a matter of fact, co-expression of pWT and pDEL vectors produced the extra-band D_B , the migration of which is faster than that of wild type and slower than that of the deleted homodimers D_A (Figure 25).

Results

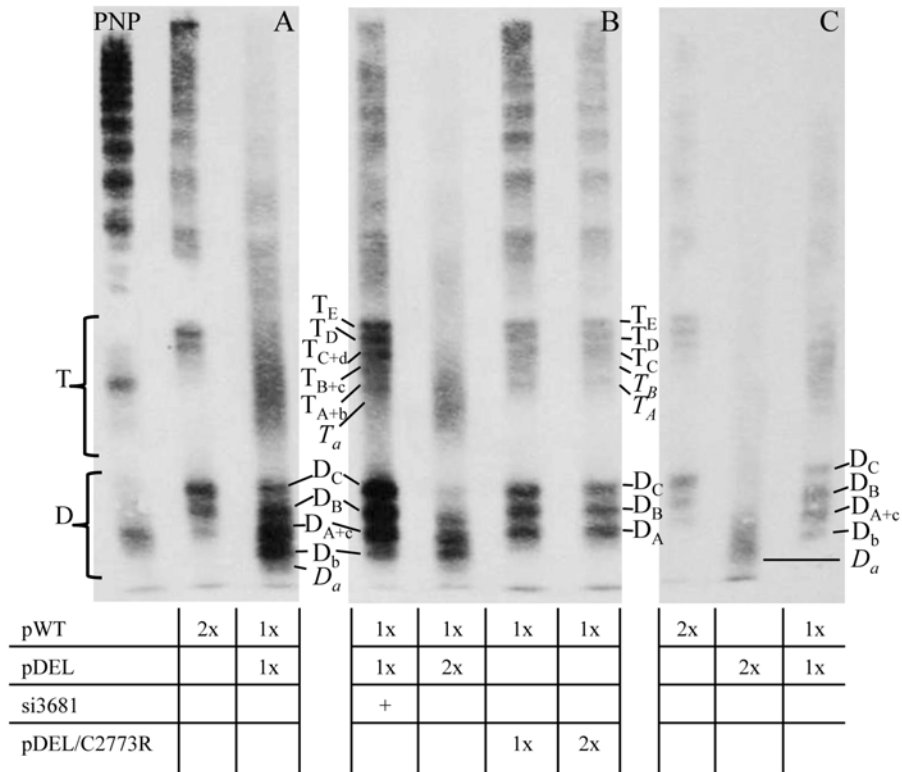


Figure 25. High resolution multimer analysis of VWF in media. Based on VWF:Ag level evaluation 1 ng of VWF was loaded in each lane (A and B). Due to the low protein concentration in media from pDEL expressing cells 0.25 ng were loaded in C, and accordingly the gel was over-exposed. PNP was diluted 1/200. The relative molar amounts of each vector and siRNA are reported in the table. Distinguishable dimers (D) and tetramers (T) are indicated together with sub-band composition (D_{A-C} and D_{a-c} ; T_{A-E} and T_{a-d}) in accordance with the schematic representation (Figure 26). Faint bands are tentatively defined and indicated in *Italics*.

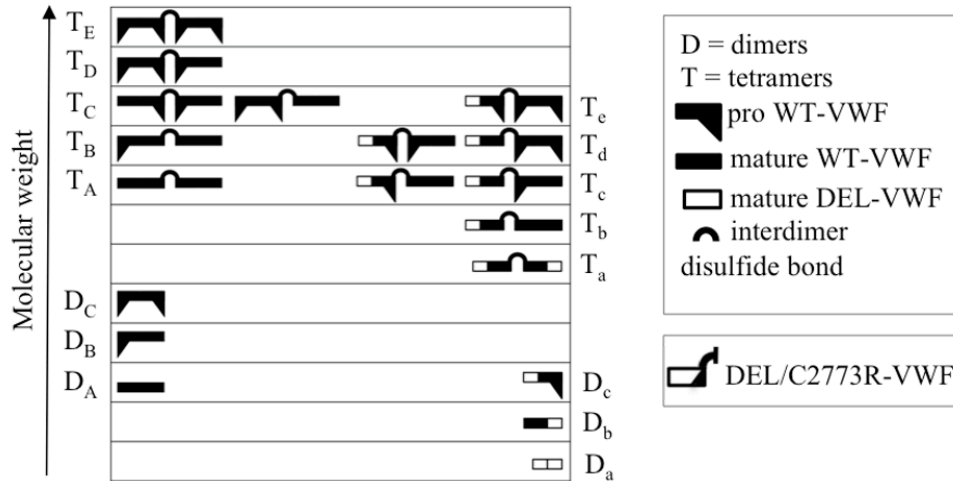


Figure 26: Schematic representation of dimers and tetramers -in accordance to Schward et al 2000¹⁰⁸ and Turecek et al 2002¹⁰⁹- reports the combinations of wild type pro- and mature-VWF (subscript uppercase letters) and mature-deleted-VWF (subscript lowercase letters). Proteins with different subunit composition but similar molecular weight, and thus co-migrating, are represented on the same line. For the sake of clarity the DEL/C2773R VWF monomer, which is not expected to form polymers, is reported at the bottom of the scheme.

The comparison between media from pWT and pWT+pDEL expressing cells in the tetramer region (T) enabled us to gain additional information about heterodimer polymerization. The fast-migrating and smeared band observed after expression of both vectors supported the presence of a number of heterotetramers, which could stem from the combination among pro-wild type, mature wild type and mature deleted VWF.

Immunofluorescence staining of intact cells was used to investigate the biosynthesis and intracellular localization of normal and deleted protein, and the dominant-negative effect of the altered VWF. Transfected cells were stained with polyclonal anti-human VWF antibodies and monoclonal antibodies directed to specific markers of subcellular compartments. Antibodies recognizing the protein disulfide isomerase and the Mannose 6-phosphate receptor were used to investigate endoplasmic reticulum and late endosomes¹¹⁰, respectively. In the first compartment, we did not detect differences in the fluorescence patterns between the wild type and in-frame deleted VWF expressing cells (Figure 27).

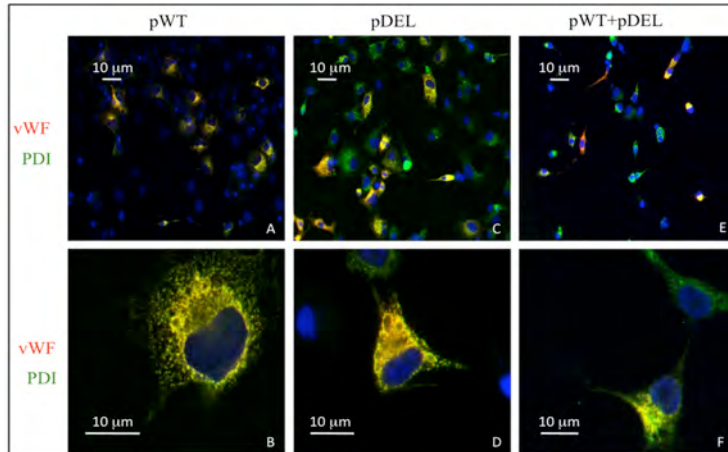


Figure 27: Intracellular distribution of recombinant VWF in the ER. Cells transfected with the vectors indicated above the images (A-F) were co-immunostained for VWF (TRITC, red) and protein disulfide isomerase (FITC, green) as ER marker. Images were acquired with Nikon Eclipse 50i equipped with DS-5M digital camera, DS-L1 control unit and Nikon Plan 20x/0.5, 40x/0.75 and Nikon 100x/0.5-1.25 Oil Iris objectives. Images were taken at room temperature on fixed cells mounting in glycerol/1,4 diazabicyclo[2.2.2]octane/DAPI medium.

Differently, the analysis of late endosomes (Figure 28) revealed that the degree of overlapping between the VWF (red)- and Mannose 6-phosphate receptor (green)-specific fluorescence was i) high in cells expressing the pWT vector (panels A-B), ii) barely detectable in cells expressing the pDEL (C-D), and iii) intermediate in cells expressing both vectors (E-F). Although the deleted protein was inefficiently transported to the late endosome compartment, the strong red fluorescence in pDEL expressing cells (C-D) indicated that the protein was efficiently synthesized, in accordance with data obtained in the reticulum (Figure 27), with Western Blot analysis (Figures 23 and 24B) and with ELISA antigen assay on cell lysates (Figure 29).

Results

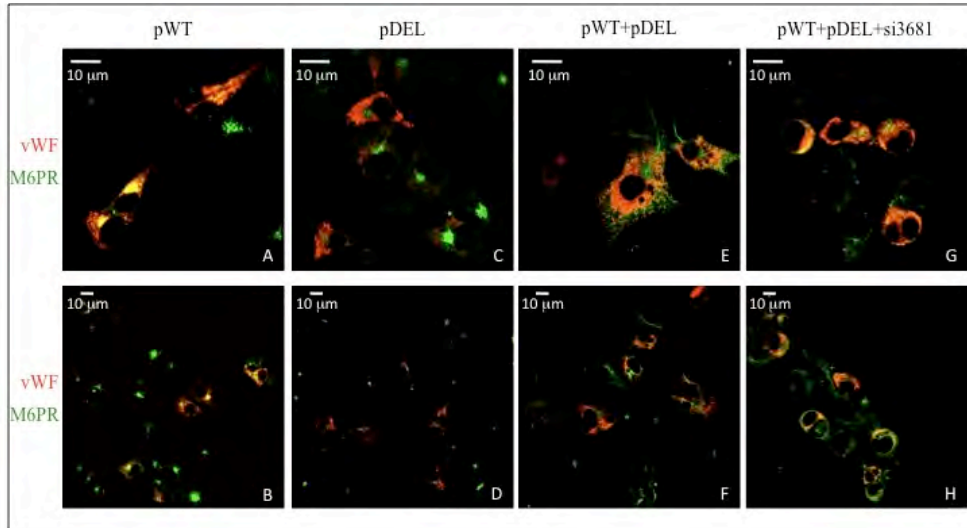


Figure 28: Intracellular distribution of recombinant VWF in late endosome compartment. Cells transfected with the vectors indicated above the images (A-H) were co-immunostained for VWF (TRITC, red) and mannose 6-phosphate receptor (FITC, green) as late endosome marker. Images were taken with Carl Zeiss LSM 510 equipped with a Fluor 40x/1.3 oil immersion objective at room temperature on fixed cells mounting in glycerol/1,4 diazabicyclo[2.2.2]octane/DAPI medium. The superimposition of red and green fluorescence not specifically due to co-localization was excluded as described in materials and methods. Images in the upper panels were digitally zoomed in twice the original size with the LSM examiner software (Carl Zeiss, Arese, Italy).

Immunofluorescence microscopy experiments did not suggest accumulation of the deleted protein inside co-transfected cells, an observation confirmed by Western blots and VWF antigen levels of cell lysates.

VWF:Ag levels in cell lysates (Figure 29) of pWT and pWT+pDEL expressing cells were not significantly different in spite of a remarkable decrease of VWF:Ag levels in conditioned media due to the addition of the pDEL vector. These observation was also true comparing pWT and pDEL or pWT and pWT+2xpDEL expressing cells.

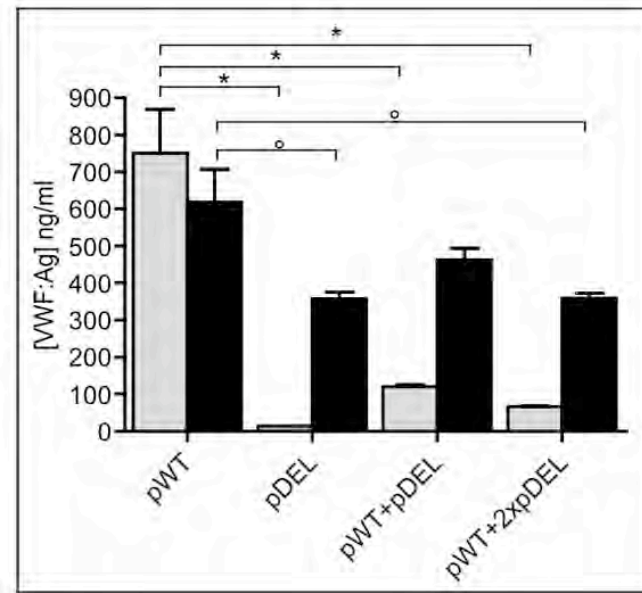


Figure 29: VWF:Ag evaluation in conditioned media (grey bars) and in cell lysates (black bars). Results of five independent experiments are reported as Mean \pm SEM. Statistical significance ($^{\circ}P < 0.01$; $*P < 0.001$) was evaluated by one-way ANOVA with Bonferroni post-test.

Taken together these experiments demonstrated the ability of the in-frame deleted VWF to interact with wild type VWF in the biosynthetic process, thus producing quantitative and qualitative alteration of secreted VWF, and particularly the impairment of HMWM formation.

Interfering with dimerization of the in-frame deleted protein by a natural mutation affecting VWF dimerization (C2773R)

A key step for the dominant-negative effect is the ability of the in-frame deleted protein to form heterodimers with the wild type VWF. To investigate the interaction between the deleted and wild type protein we exploited natural missense changes interfering with VWF dimerization (type 2A IID VWD)^{111,112}, and among those the C2773R²³. Cysteine 2773 was also selected because molecular modelling and expression of norrin have supported its key role in dimerization through intersubunit disulfide bond formation²⁴. The insertion of this missense change in the double mutant vector pDEL/C2773R (Material and Methods, Figure 13) was aimed at

impairing dimerization of the deleted VWF, when co-expressed with the wild type protein.

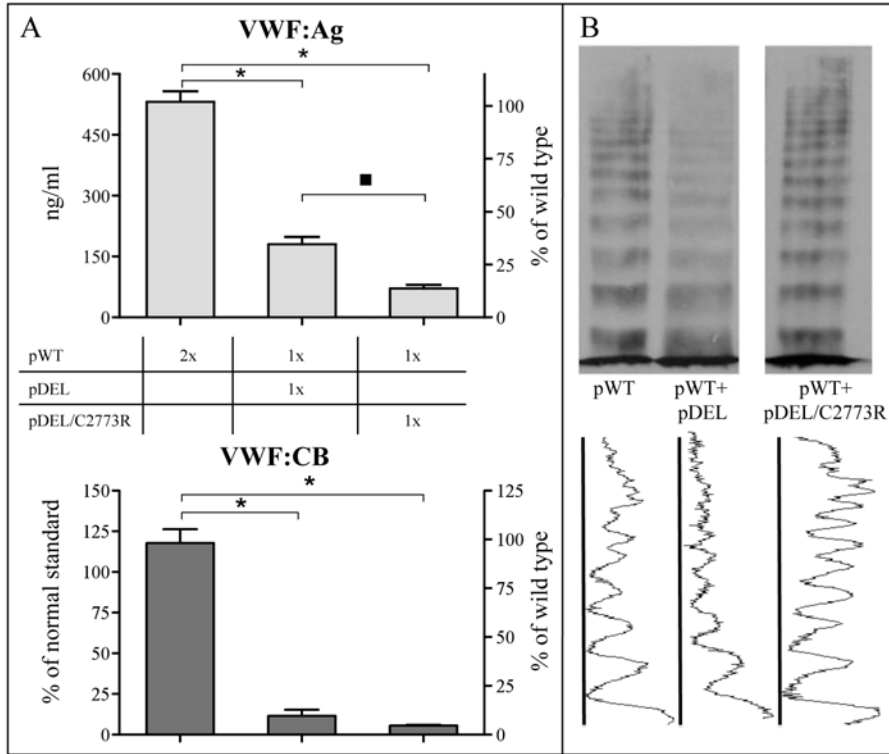


Figure 30: Dominant-negative effect of the double mutant pDEL/C2773R VWF variant. (A) VWF:Ag (upper panel) and VWF:CB (lower panel) levels in conditioned media. The relative molar amounts of pWT, pDEL and pDEL/C2773R vectors are reported in the table. Statistical significance (* $P < 0.001$; ■ $P < 0.05$) and analysis as in Figure 22. The right y axis indicates the percentage of wild type (100% VWF:Ag, 531.7 ng/ml; 100% VWF:CB, 117.9 of normal standard) (B) Multimer pattern and densitometric profile (GS 700 Imaging Densitometer and Quantity One® software, Bio-Rad). 1.7 ng of VWF was loaded in each lane.

Comparison of media from cells co-transfected with pWT + pDEL or pWT + pDEL/C2773R (Figure 30A) indicated that the combination of the deletion and point mutation produced low antigen levels ($13.6 \pm 2.7\%$ of wild type) and appreciable collagen-binding activity ($4.9 \pm 0.7\%$ of wild type). On the other hand, multimer patterns obtained by loading equal amounts of VWF

(Figure 30B) revealed that the relative amounts of HMWMs produced by the pWT +pDEL/C2773R co-transfection appeared indistinguishable from that of wild type. These findings were further detailed by multimer analysis performed in high resolution gels (Figure 25B). Cells expressing the pWT + pDEL/C2773R vectors produced normal oligomers (D_{A-B-C} and $T_{A-B-C-D-E}$) and did not secrete detectable amounts of heterodimers or heterotetramers. Moreover, the wild type, mature homodimers (D_A) were better represented in these cells than in those expressing the pWT vector only (Figure 25A, B). It appeared that, in co-transfected COS cells, the propeptide cleavage of the normal protein was relatively improved in the presence of the double mutant VWF, and of the consequent slowdown of the VWF biosynthetic process.

Taken together co-expression experiments supported the notion that reducing the efficiency of heterodimer formation, mediated by the C2773R change in the in-frame deleted VWF molecules, relatively improves the ability of wild type VWF to produce HMWMs.

Interfering with dimerization of the in-frame deleted protein by RNA silencing - Correction strategy

We investigated whether siRNAs (Material and Methods, Figure 13), specifically directed to the VWF mRNA breakpoint in the pDEL, were able to rescue wild type VWF biosynthesis and secretion.

To find the most selective and efficient silencing molecules we tested in preliminary experiments two siRNAs complementary to the breakpoint sequence. Evaluation at the VWF mRNA level by RT-PCR and denaturing capillary electrophoresis led us to select the si3681 molecule, which at 40nM was able to substantially and selectively decrease the deleted VWF mRNA level (Figure 31A).

The positive effects of the si3681 were detectable in the fluorescence pattern of treated cells, which appeared similar to that of wild type VWF expressing cells (Figure 28, panels G-H vs A-B).

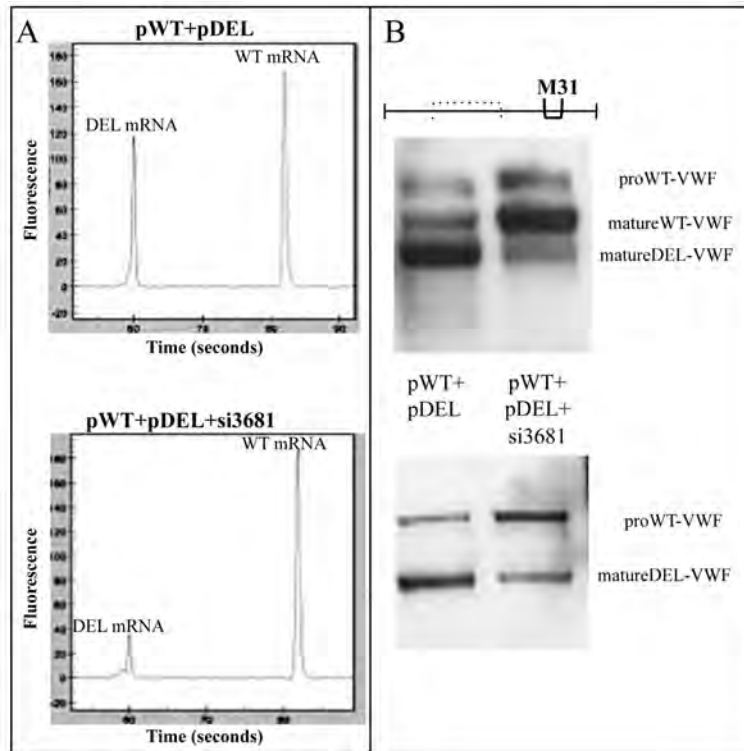


Figure 31. Counteracting the dominant-negative effect by allele specific silencing. (A) Wild type and deleted mRNA before and after si3681 treatment detected by capillary electrophoresis of RT PCR products. (B) Western blot analysis of conditioned media (upper panel) and cell lysates (lower panel) with M31 antibody pool.

Western blotting results (Figure 31B) demonstrated at the protein level that the silencing treatment substantially modified the proportion between secreted wild type and deleted molecules, favouring the wild type. This occurred both in the extracellular space (Figure 31B, upper panel) and in the intracellular compartments (Figure 31B, lower panel). The densitometric analysis indicates that the ratios between the altered and normal VWF decreased from 3.5 to 0.5 in lysates, and from 1.8 to 0.3 in media respectively. The si3681 treatment produced a three-fold increase in antigen levels (up to 74.8 ± 5.0 % of wild type, Figure 31C, upper panel). Moreover, the collagen-binding activity, undetectable before the treatment, improved to 28.0 ± 3.3 % of wild type (Figure 31C, lower panel). As control the si3681 did not influence (VWF:Ag, 96.5%) wild type expression.

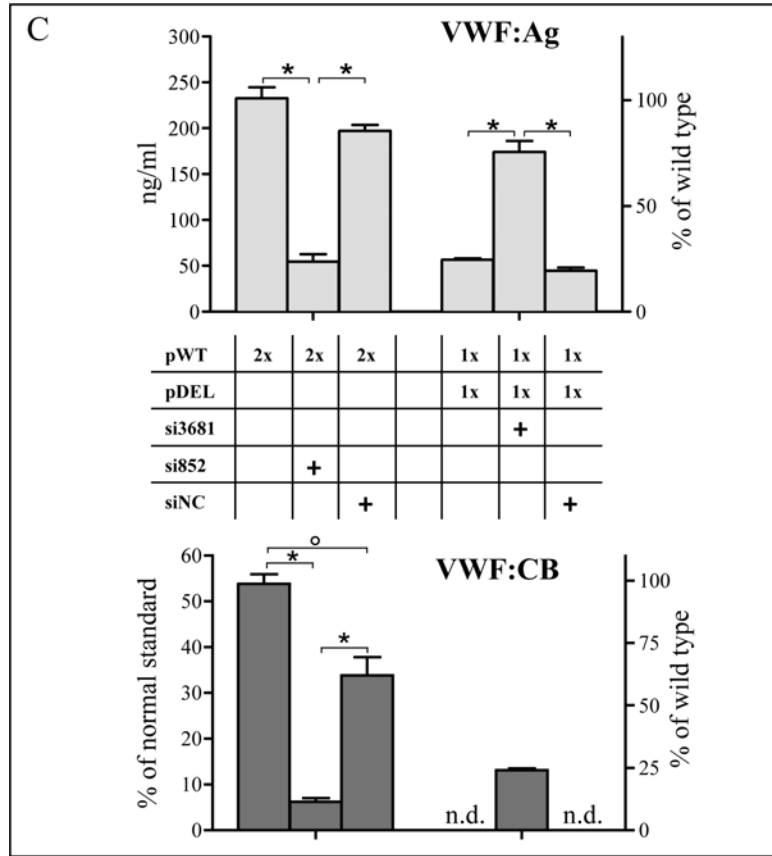


Figure 31(C): VWF:Ag and VWF:CB levels and from conditioned media. The relative molar amount of pWT and pDEL vectors, and concentration of siRNAs are reported in the tables. Statistical significance (* $P < 0.001$; ° $P < 0.01$) and analysis as in Figure 22. The right y axis indicates the percentage of wild type (100% VWF:Ag, 233.0 ng/ml; 100% VWF:CB, 53.8 % of normal standard).

Moreover, a negative control siRNA (siNC) did not induce appreciable alterations of VWF levels in pWT+pDEL expression and a positive control (si852), appropriately designed to silence the expression of wild type VWF, produced a quantitative defect characterized by markedly reduced VWF:Ag and VWF:CB levels ($P < 0.001$). No changes in cell morphology or cell density were observed by bright-field microscopy after siRNA treatment (not shown).

The si3681-mediated amelioration of antigen and collagen-binding activity in media of co-transfected cells were reflected in the increase in amount of

HMWMs (Figure 31D). Moreover, the high resolution gels (Figure 25B) indicated that the bands containing wild type homodimers (D_{B-C}) and homotetramers (T_{D-E}) were increased in intensity. Taken together these data support both quantitative and qualitative improvement induced by the siRNA treatment.

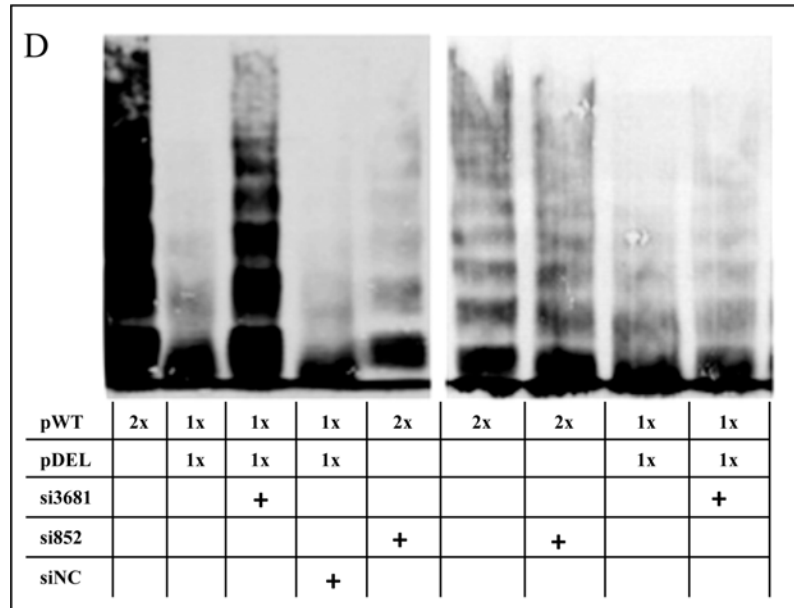


Figure 31(D): Multimer analysis of condition media from transiently transfected cells. Left panel, equal volume of media; right panel, equal amount of VWF (1.7 ng). The relative molar amount of vectors and siRNAs were indicated in the table.

GENERAL DISCUSSION

The definition of the molecular mechanisms leading to the dominant inheritance of most VWD types is a key step to understanding the disease pathophysiology, which has a major role in determining its prevalence, and requires mutation-based cellular models.

The cellular model of the heterozygous and in-frame deletion under study represents a valuable tool to investigate the dominant-negative mechanism hypothesized⁶ to be responsible for a severe type 2 VWD form. The design and expression of recombinant vectors enabled us to evaluate through several methodological approaches the main biosynthetic steps of the deleted protein, and its interaction with wild type VWF. Improved knowledge of the detrimental properties of the altered protein led us to propose and explore strategies to counteract its effects.

Noticeably, conditioned media from cells expressing the deleted and wild type mRNA closely mirrored the severe defect observed in patient plasma. In spite of the limitation imposed by cell culture model, striking similarity was detectable for protein amounts (VWF:Ag, $19.7 \pm 0.7\%$ vs 24), quality (virtual absence of HMWMs) and thus function (VWF:CB, $2.9 \pm 0.7\%$ vs VWF:RCo, 3%). These results were consistent with the presence of a particularly efficient dominant-negative mechanism, the molecular bases of which were investigated in relation to deleted monomer expression, dimer and multimer formation, propeptide cleavage and subcellular localization of VWF.

In cells transfected with the deleted construct, the altered mRNA was efficiently translated, as indicated by the large amounts of the deleted VWF in cell lysates. Inside co-transfected cells, the deleted protein was much more represented than the wild type form, which would potentiate the dominant-negative effect of the altered molecules. In addition, the quantity of the deleted protein appeared to be higher in conditioned media of cells co-expressing wild type VWF than of those transfected with the pDEL vector only.

Formation of dimers between normal and deleted VWF (heterodimers), which should play a key role in the dominant-negative behaviour, would be sustained by the “cysteine knot” domain, a motif localised at the carboxyl-terminus of the protein^{20,113} that was correctly encoded in the deleted VWF. As a matter of fact, our analysis of conditioned media in high resolution gels indicated the presence of heterodimers and of deleted homodimers, thus implying both a properly folded domain and its ability to participate in the process. The absence of

all A domains does not limit dimerization, in accordance with the notion that these modules are not involved in the process, and with features and evolution of A domain-containing proteins⁵⁷.

On the other hand, formation of multimers containing the deleted protein should be impaired in the absence of the D3 sequence C1222-C1227, containing the Cys residue responsible for the inter-dimer disulfide bond^{22,93,94}. Whereas deleted homodimers cannot sustain any subsequent polymerization step (Figure 32), the heterodimer can ensure only an asymmetric multimerization giving rise to heterotetramers, which were detected in high resolution gels. According to their ability to form only one disulfide bond with pre-existing dimers or multimers, the heterodimer could act as terminator^{99,111} of the multimerization process (Figure 32). The multimer pattern, and the abundance of the deleted VWF in Western blots of media from co-transfected cells, support the presence of remarkable amounts of terminated LMWMs, which do not contain unpaired bands due to the efficient dimerization of altered molecules.

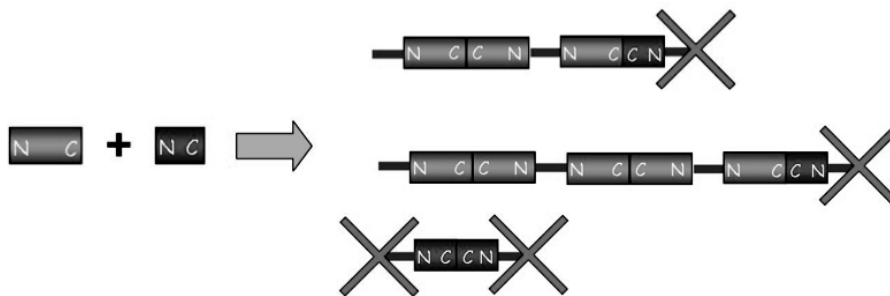


Figure 32: Schematic representation of the termination mechanism. The deleted monomer can dimerize through its normal C-terminal end but cannot multimerize through its N-terminal extremity. A dimer containing two deleted monomers cannot further polymerize. When a heterodimer is added to a growing polymer it stops the multimerization process at the selected extremity.

Impairment of multimer formation by heterodimers is further sustained by expression experiments with a double mutant vector, containing both the deletion and the C2773R change, a well described mutation that prevents dimerization^{23,111}. By co-expressing wild type and double mutant vectors we expected to decrease the dominant-negative effect of the deletion, and to transform a qualitative VWD form in a quantitative defect, characterized by similarly reduced antigen and activity levels. Accordingly, the observed

multimeric pattern showed a relative proportion of HMWMs indistinguishable from normal. This feature, and the virtually exclusive presence of normal oligomers in high resolution gels, indicate that the C2773R mutation, preventing heterodimer formation, shifts the equilibrium towards wild type HMWMs. On the other hand the double mutant maintains a dominant negative character as indicated by the remarkable reduction in antigen levels.

The multimerization and propeptide cleavage steps are catalysed by independent enzymatic activities²⁹⁻³², the efficiency of which can be compared for the deleted and wild type VWF. Since pro-deleted VWF is barely detectable within cells and undetectable in media, dimers containing the deleted protein appear to be preferentially cleaved by furin-like endopeptidase activity²⁹ as compared with wild type dimers. Although the genuine nature of this observation cannot be established in COS cells, both structural features of the deleted VWF, and increased residence time in endopeptidase-containing compartments, could favour protein cleavage. As a consequence, the poor attitude of the deleted VWF to multimerize was coupled with complete propeptide proteolysis at the intracellular level.

Multimers are either secreted or stored in Weibel Palade bodies that cannot be investigated in COS cells²⁵. However, the cellular model under study provides some information about the intracellular localization of VWF, and potentially to accumulation of abnormal proteins, which would contribute to the decreased amount of secreted molecules. As determined by cell immunostaining, late endosomes of cells expressing a single construct contained higher amounts of wild type than deleted VWF, in accordance with the low amount of altered protein in media. Coherently, co-transfected cells displayed an intermediate amount of VWF in this compartment.

Neither in transfection nor in co-transfection experiments we obtained evidence for sites of intracellular accumulation. As comparison, the extensively studied dominant-negative C1149R mutation resulted in intracellular retention of mutant molecules¹¹⁴⁻¹¹⁶, suggesting that intracellular removal would be more efficient for the deleted than for the missense VWF variant.

Overall data provide experimental evidence for a series of coherent features, which pertain to the molecular mechanism of the observed dominant-negative effects:

- i) the deleted protein is synthesized and folded in large amounts, and is preferentially processed
- ii) the deleted protein exhibits a correct C-terminal end and thus efficiently forms altered homodimers and heterodimers with wild type VWF (Figure 32), the last prevailing in media of co-transfected cells
- iii) the heterodimers would be modestly affected by the quality control in the endoplasmic reticulum, which would favour their role as terminator molecules^{99,111} of the multimerization process (Figure 32) in the Golgi compartment
- iv) reduced amounts of VWF are detectable in the late endosome compartment and secreted as LMWMs.

To further investigate the dominant-negative molecular mechanism of the deletion, and to suppress its effects, we successfully used a silencing approach^{117,118}, selectively targeting the deleted RNA. This is an original attempt aimed at correcting VWD phenotype, albeit at the cellular level.

Although targeting of the siRNAs was limited by the short and obliged sequence of the breakpoint region, where exon 25 and 35 are joined, we devised an efficient molecule that significantly decreased the amount of the deleted VWF mRNA. Since reduced amount of the deleted mRNA persisted after RNAi treatment, VWF function was largely improved but not completely restored.

By removing the effects of the deleted construct, the results of the RNA interference formally validate the presence of the dominant-negative mechanism: the reduced availability of the deleted mRNA and protein decreased the rate of heterodimer formation. As a consequence the treatment resulted in i) increased availability of mature wild type VWF, ii) appearance of HMWMs in media of treated cells and iii) increase of the collagen-binding activity.

Although these novel findings have to be confirmed in patient's cells, they pave the way to an *in vivo* application aimed at curing¹¹⁹ the unique patient under study and, because dominant-negative mechanisms are shared with others diseases, at devising correction strategies for other genetic conditions.

REFERENCES

References

1. Furie B, Furie BC. The molecular basis of blood coagulation. *Cell*. 1988;53: 505-518.
2. Pearson JD. Endothelial cell function and thrombosis. *Baillieres Best Pract Res Clin Haematol*. 1999;12(3):329-41.
3. Arnout J, Hoylaerts MF, Lijnen HR. Haemostasis. *Handb. Exp. Pharmacol.* 2006;(176 Pt 2):1-41.
4. Rojkaer LP Clot stabilization for the prevention of bleeding. *Hematol Oncol. Clin North Am*. 2007;21:25-32
5. Cesarman-Maus G, Hajjar K.A. Molecular mechanisms of fibrinolysis. *Br.J Haematol*. 2005;129(3):307-21.
6. Riddel JP, Aouizerat BE, Miaskowski C, Lillicrap DP. Theories of blood coagulation. *J Pediatr Oncol Nurs*. 2007;24(3):123-31.
7. Sadler J.E. Biochemistry and genetics of von Willebrand factor. *Annual Review of Biochemistry*. 1998;67: 395-424.
8. Noe DA. A mathematical model of coagulation factor VIII kinetics. *Haemostasis*. 1996;26(6):289-303.
9. Schambeck CM, Grossmann R, Zonnur S, Berger M, Teuchert K, Spahn A, Walteret U. High factor VIII (FVIII) levels in venous thromboembolism: role of unbound FVIII. *Thromb.Haemost*. 2004;92(1): 42-46.
10. Federici AB. The factor VIII/von Willebrand factor complex: basic and clinical issues. *Haematologica*. 2003;88(6):3-12.
11. Lenting PJ, van Mourik JA, and Mertens K. The life cycle of coagulation factor VIII in view of its structure and function. *Blood*. 1998;92(11): 3983-3996.
12. Haberichter SL, Shi Q, Montgomery RR. Regulated release of VWF and FVIII and the biologic implications. *Pediatr Blood Cancer*. 2006;46(5): 547-553.
13. Nachman R, Levine R, Jaffe EA. Synthesis of factor VIII antigen by cultured guinea pig megakaryocytes. *J Clin Invest*. 1977;60(4):914-921.
14. Jaffe EA, Hoyer LW, Nachman RL. Synthesis of antihemophilic factor antigen by cultured human endothelial cells. *J Clin Invest*. 1973;52(1): 2757-2764.

References

15. Ginsburg D, Handin RI, Bonthron DT, Donlon TA, Bruns GA, Latt SA, Orkin SH. Human von Willebrand factor (vWF): isolation of complementary DNA (cDNA) clones and chromosomal localization. *Science*. 1985;228(4706):1401-6
16. Kuwano A, Morimoto Y, Nagai T, Fukushima Y, Ohashi H, Hasegawa T, Kondo I. Precise chromosomal locations of the genes for dentatorubral-pallidoluysian atrophy (DRPLA), von Willebrand factor (F8vWF) and parathyroid hormone-like hormone (PTH LH) in human chromosome 12p by deletion mapping. *Hum Genet*. 1996;97(1):95-8
17. Patracchini P, Calzolari E, Aiello V, Palazzi P, Banin P, Marchetti G, Bernardi F. Sublocalization of von Willebrand factor pseudogene to 22q11.22-q11.23 by in situ hybridization in a 46,X,t(X;22)(pter;q11.21) translocation. *Hum Genet*. 1989;83(3):264-6
18. Marchetti G, Patracchini P, Volinia S, Aiello V, Schiavoni M, Ciavarella N, Calzolari E, Schwienbacher C, Bernardi F. Characterization of the pseudogenic and genic homologous regions of von Willebrand factor. *Br J Haematol*. 1991;78(1):71-9
19. Wagner DD. Cell biology of von Willebrand factor. *Annu Rev Cell Biol*. 1990:217-46
20. Katsumi A, Tuley EA, Bodò I, Sadler JE. Localization of disulfide bonds in the cystine knot domain of human von Willebrand factor. *J Biol Chem*. 2000;275(33):25585-25594.
21. Marti T, Rosselet SJ, Titani K, Walsh KA. Identification of disulfide-bridged substructures within human von Willebrand factor. *Biochemistry*. 1987;26(25):8099-8109.
22. Dong Z, Thoma RS, Crimmins DL, McCourt DW, Tuley EA, Sadler JE. Disulfide bonds required to assemble functional von Willebrand factor multimers. *J Biol Chem*. 1994;269(9): 6753-6758.
23. Schneppenheim R, Brassard J, Krey S, Budde U, Kunicki TJ, Holmberg L, Ware J, Ruggeri ZM. Defective dimerization of von Willebrand factor subunits due to a Cys-> Arg mutation in type IID von Willebrand disease. *Proc Natl Acad Sci USA*. 1996;93(8):3581-6
24. Sadler JE. Von Willebrand factor assembly and secretion. *J Thromb Haemost*. 2009;7(Suppl 1):24-7

References

25. Wagner DD, Saffaripour S, Bonfanti R, Sadler JE, Cramer EM, Chapman B, Mayadas TN. Induction of specific storage organelles by von Willebrand factor propolypeptide. *Cell*. 1991;64(2):403-413.
26. Titani K., Kumar S., Takio K, Ericsson LH, Wade RD, Ashida K, Walsh KA, Chopek MW, Sadler JE, Fujikawa K. Amino acid sequence of human von Willebrand factor. *Biochemistry*. 1986;25(11): 3171-3184.
27. Samor B, Michalski JC, Mazurier C, Goudemand M, De Waard P, Vliegthart JF, Strecker G, Montreuil J. Primary structure of the major O-glycosidically linked carbohydrate unit of human von Willebrand factor. *Glycoconj J*. 1989;6(3):263-270.
28. Vlot AJ, Koppelman SJ, Bouma BN, Sixma JJ. Factor VIII and von Willebrand factor. *Thromb.Haemost*. 1998;79(3):456-465.
29. Verweij CL, Hart M, Pannekoek H. Proteolytic cleavage of the precursor of von Willebrand factor is not essential for multimer formation. *J Biol Chem*. 1988;263(17):7921-4
30. Voorberg J, Fontijn R, van Mourik JA, Pannekoek H. Domains involved in multimer assembly of von willebrand factor (vWF): multimerization is independent of dimerization. *EMBO J*. 1990;9(3):797-803
31. Mayadas TN, Wagner DD. Vicinal cysteines in the prosequence play a role in von Willebrand factor multimer assembly. *Proc Natl Acad Sci USA*. 1992;89(8):3531-5
32. Rehemtulla A, Kaufman RJ. Preferred sequence requirements for cleavage of pro-von Willebrand factor by propeptide-processing enzymes. *Blood*. 1992; 79(9):2349-55.
33. Purvis AR and Sadler JE. A covalent oxidoreductase intermediate in propeptide-dependent von Willebrand factor multimerization. *J.Biol.Chem*. 2004;279(48): 49982-49988.
34. Wagner DD, Mayadas T, Marder VJ. Initial glycosylation and acidic pH in the Golgi apparatus are required for multimerization of von Willebrand factor. *J Cell Biol*. 1986;102(4):1320-1324.
35. van Mourik JA, Thalia Romani de Wit, Voorberg J. Biogenesis and exocytosis of Weibel-Palade bodies. *Histochem Cell Biol*. 2002;117(2): 113-22
36. Michaux G, Cutler DF. How to roll an endothelial cigar: the biogenesis of Weibel-Palade bodies. *Traffic*. 2004;5(2):69-78

References

37. Rondaij MG, Bierings R, Kragt A, van Mourik JA, Voorberg J. Dynamics and plasticity of Weibel-Palade bodies in endothelial cells. *Arterioscler Thromb Vasc Biol.* 2006;26(5):1002-7
38. Verweij CL. Biosynthesis of human von Willebrand factor. *Haemostasis.* 1988;18(4-6):224-45
39. de Wit TR, van Mourik JA. Biosynthesis, processing and secretion of von Willebrand factor: biological implications. *Best Pract Res Clin Haematol.* 2001;14(2):241-55
40. Reininger AJ. Function of von Willebrand factor in haemostasis and thrombosis. *Haemophilia.* 2008;14(Suppl 5):11-26.
41. Wagner DD, Fay PJ, Sporn LA, Sinha S, Lawrence SO, Marderet VJ. Divergent fates of von Willebrand factor and its propolypeptide (von Willebrand antigen II) after secretion from endothelial cells. *Proc Natl Acad Sci USA.* 1987;84(7):1955-9.
42. Haberichter SL, Fahs SA, Montgomery RR. von Willebrand factor storage and multimerization: 2 independent intracellular processes. *Blood.* 2000;96(5):1808-15
43. Gill JC, Endres-Brooks J, Bauer PJ, Marks W J, Montgomery RR. The effect of ABO blood group on the diagnosis of von Willebrand disease. *Blood.* 1987;69(6):1691-5.
44. Matsui T, Fujimura Y, Nishida S, Titani K. Human plasma alpha 2-macroglobulin and von Willebrand factor possess covalently linked ABO(H) blood group antigens in subjects with corresponding ABO phenotype. *Blood.* 1993;82(2):663-8
45. Orstavik KH, Magnus P, Reisner H, Berg K, Graham JB, Nance W. Factor VIII and factor IX in a twin population. Evidence for a major effect of ABO locus on factor VIII level. *Am J Hum Genet.* 1985;37(1):89-101
46. Vlot AJ, Mauser-Bunschoten EP, Zarkova AG, Haan E, Kruitwagen CL, J J Sixma JJ, van den Berg HM. The half-life of infused factor VIII is shorter in hemophiliac patients with blood group O than in those with blood group A. *Thromb Haemost.* 2000;83(1):65-9
47. Yamamoto F. Review: ABO blood group system--ABH oligosaccharide antigens, anti-A and anti-B, A and B glycosyltransferases, and ABO genes. *Immunohematology.* 2004;20(1):3-22.

References

48. Dent JA, Galbusera M, and Ruggeri ZM. Heterogeneity of plasma von Willebrand factor multimers resulting from proteolysis of the constituent subunit. *J Clin Invest.* 1991;88(3):774-82
49. Zheng X, Chung D, Takayama TK, Majerus EM, Sadler JE, Fujikawa K. Structure of von Willebrand factor-cleaving protease (ADAMTS13), a metalloprotease involved in thrombotic thrombocytopenic purpura. *J Biol Chem.* 2001;276(44):41059-63
50. Fujikawa K, Suzuki H, McMullen, Chung D. Purification of human von Willebrand factor-cleaving protease and its identification as a new member of the metalloproteinase family. *Blood.* 2001;98(6):1662-698.
51. Zheng X, Majerus EM, Sadler JE. ADAMTS-13 and TTP. *Curr Opin Hematol.* 2002; 9(5):389-94
52. Chow TW, Turner NA, Chintagumpala M, McPherson PD, Nolasco LH, Rice L, Hellums JD, Moake JL. Increased von Willebrand factor binding to platelets in single episode and recurrent types of thrombotic thrombocytopenic purpura. *Am J Hematol.* 1998;57(4):293-302
53. Dong JF, Moake JL, Nolasco L, Bernardo A, Arceneaux W, Shrimpton CN, Schade AJ, McIntire LV, Fujikawa K, López JA. ADAMTS-13 rapidly cleaves newly secreted ultralarge von Willebrand factor multimers on the endothelial surface under flowing conditions. *Blood.* 2002;100(12):4033-9
54. Padilla A, Moake JL, Bernardo A, Ball C, Wang Y, Arya M, Nolasco L, Turner N, Berndt MC, Anvari B, López JA, Dong J-F. P-selectin anchors newly released ultralarge von Willebrand factor multimers to the endothelial cell surface. *Blood.* 2004;103(6):2150-6
55. Michaux G, Pullen TJ, Haberichter SL, Cutler DF. P-selectin binds to the D'-D3 domains of von Willebrand factor in Weibel-Palade bodies. *Blood.* 2006;107(10):3922-4
56. Ruggeri, ZM, Ware JL, Ginsburg D. Von Willebrand factor. IN: *Thrombosis and Hemorrhage.* Third Edition. Loscalzo, J. and Schafer, A.I., eds., Lippincott, Williams & Wilkins, Baltimore, 2002 pp. 246-265,.
57. Whittaker CA, Hynes. Distribution and evolution of von Willebrand/ integrin A domains: widely dispersed domains with roles in cell adhesion and elsewhere. *Mol Biol Cell.* 2002;13(10):3369-87
58. Nichols WL, Hultin MB, James AH et al. Von Willebrand disease (VWD): evidence-based diagnosis and management guidelines, the National

References

- Heart, Lung, and Blood Institute (NHLBI) Expert Panel report (USA).
Haemophilia 2008;14:171-232
59. von Willebrand EA. Hereditär pseudoheemofili. Finska Läkarsällskapetets Handlingar. 7-112, 1926.
60. Schneppenheim R, Budde U, Ruggeri ZM. A molecular approach to the classification of von Willebrand disease. Best Practice & Research Clinical Haematology. 2001;14(2):281-98.
61. Sadler JE, Budde U, Eikenboom JCJ et al. Update on the pathophysiology and classification of von Willebrand disease: a report of the Subcommittee on von Willebrand Factor. J Thromb Haemost. 2006;4(10):2103-14
62. Lillicrap D. Von Willebrand disease-Phenotype versus genotype: Deficiency versus disease. Thromb Res. 2007;120(Suppl 1):S11.
63. Sadler JE. Von Willebrand disease type 1: a diagnosis in search of a disease. Blood. 2003;101(6):2089-93.
64. Sadler JE. New concepts in von Willebrand disease. Annu Rev Med. 2005;56:173-91.
65. Ngo KY, Glotz VT, Koziol JA, Lynch DC, Gitschier J, Ranieri P, Ciavarella N, Ruggeri ZM, Zimmerman TS. Homozygous and heterozygous deletions of the von Willebrand factor gene in patients and carriers of severe von Willebrand disease. Proc Natl Acad Sci USA. 1988;85(8):2753-7.
66. Eikenboom JC, Ploos van Amstel HK, Reitsma PH, Briët E. Mutations in severe, type III von Willebrand's disease in the Dutch population: candidate missense and nonsense mutations associated with reduced levels of von Willebrand factor messenger RNA. Thromb Haemost. 1992;68(4):448-54.
67. Weiss HJ, Ball AP, Mannucci PM. Incidence of severe von Willebrand's disease. N Engl J Med. 1982;307(2):127.
68. Goodeve A, Eikenboom J, Castaman G, Rodeghiero F, Federici AB, Batlle J, Meyer D, Mazurier C, Goudemand J, Schneppenheim R, Budde U, Ingerslev J, Habart D, Vorlova Z, Holmberg L, Lethagen S, Pasi J, Hill F, Sotah MH, Baronciani L, Hallden C, Guilliatt A, Lester W, Peake I. Phenotype and genotype of a cohort of families historically diagnosed with type 1 von Willebrand disease in the European study, Molecular and Clinical Markers for the Diagnosis and Management of

References

- Type 1 von Willebrand Disease (MCMDM-1VWD). *Blood*. 2007;109(1):112-21.
69. James PD, Notley C, Hegadorn C, Leggo J, Tuttle A, Tinlin S, Brown C, Andrews C, Labelle A, Chirinian Y, O'Brien L, Othman M, Rivard G, Rapson D, Hough C, Lillicrap D. The mutational spectrum of type 1 von Willebrand disease: Results from a Canadian cohort study. *Blood*. 2007;109(1):145-54.
70. Lyons SE, Bruck ME, Bowie EJ, Ginsburg D. Impaired intracellular transport produced by a subset of type IIA von Willebrand disease mutations. *J Biol Chem*. 1992;267(7):4424-30.
71. Dent JA, Berkowitz SD, Ware J, Kasper CK, Ruggeri ZM. Identification of a cleavage site directing the immunochemical detection of molecular abnormalities in type IIA von Willebrand factor. *Proc Natl Acad Sci USA*. 1990;87(16):6306-10.
72. Ruggeri ZM, Pareti FI, Mannucci PM, Ciavarella N, Zimmerman TS. Heightened interaction between platelets and factor VIII/von Willebrand factor in a new subtype of von Willebrand's disease. *N Engl J Med*. 1980;302(19):1047-51.
73. Ribba AS, Lavergne JM, Bahnak BR, Derlon A, Piétu G, Meyer D. Duplication of a methionine within the glycoprotein Ib binding domain of von Willebrand factor detected by denaturing gradient gel electrophoresis in a patient with type IIB von Willebrand disease. *Blood*. 1991;78(7):1738-43 .
74. Meyer D, Fressinaud E, Hilbert L, Ribba AS, Lavergne JM, Mazurier C. Type 2 von Willebrand disease causing defective von Willebrand factor-dependent platelet function. *Best Pract Res Clin Haematol*. 2001;14(2):349-64.
75. Meyer D, Fressinaud E, Gaucher C, Lavergne JM, Hilbert L, Ribba AS, Jorieux S, Mazurier C. Gene defects in 150 unrelated French cases with type 2 von Willebrand disease: from the patient to the gene. INSERM Network on Molecular Abnormalities in von Willebrand Disease. *Thromb Haemost*. 1997;78(1):451-6.
76. Nishino M, Girma JP, Rothschild C, Fressinaud E, Meyer D. New variant of von Willebrand disease with defective binding to factor VIII. *Blood*. 1989;74(5):1591-9.
77. Mazurier C, Dieval J, Jorieux S, Delobel J, Goudemand M. A new von Willebrand factor (vWF) defect in a patient with factor VIII (FVIII)

References

- deficiency but with normal levels and multimeric patterns of both plasma and platelet vWF. Characterization of abnormal vWF/FVIII interaction. *Blood*. 1990;75(1):20-6.
78. Schneppenheim R, Budde U, Krey S, Drewke E, Bergmann F, Lechler E, Oldenburg J, Schwaab R. Results of a screening for von Willebrand disease type 2N in patients with suspected haemophilia A or von Willebrand disease type 1. *Thromb Haemost*. 1996;76(4):598-602.
79. Fressinaud E, Mazurier C, Meyer D. Molecular genetics of type 2 von Willebrand disease. *Int J Hematol*. 2002;75(1):9-18
80. Kim SS, Garg H, Joshi A, Manjunath N. Strategies for targeted nonviral delivery of siRNAs in vivo. *TRENDS in Molecular Medicine*. 2009;15(11):491-500
81. Rassouli FB, Matin MM. Gene silencing in human embryonic stem cells by RNA interference. *Biochem Biophys Res Commun*. 2009; 390(4): 1106-10
82. Goyal BR, Patel MM, Soni MK, Bhadada SV. Therapeutic opportunities of small interfering RNA. *Fundam Clin Pharmacol*. 2009;23(4):367-86
83. Pelletier R, Caron SOP, Puymirat J. RNA based gene therapy for dominantly inherited diseases. *Curr Gene Ther*. 2006;6(1):131-46
84. Strachan T, Read AP. *Human Molecular Genetics* 2. Garland Science. 16.4.4. Mutations in proteins that work as dimers or multimers sometimes produce dominant negative effects.
85. Hickerson RP, Smith FJD, Reeves RE, Contag CH, Leake D, Leachman SA, Milstone LM, Mclean WHI, Kaspar RL. Single-Nucleotide-Specific siRNA Targeting in a Dominant-Negative Skin Model. *J Invest Dermatol*. 2007:1-12
86. Leachman SA, Hickerson RP, Hull PR, Smith FJD, Milstone LM, Lane EB, Bale SJ, Roop DR, McLean WHI, Kaspar RL. Therapeutic siRNAs for dominant genetic skin disorders including pachyonychia congenita. *J Dermatol Sci*. 2008;51(3):151-7
87. Bernardi F, Marchetti G, Guerra S et al. A de novo and heterozygous gene deletion causing a variant of von Willebrand disease. *Blood*. 1990;75(3):677-83

References

88. Bernardi F, Patracchini P, Gemmati D et al. In-frame deletion of von Willebrand factor A domains in a dominant type of von Willebrand disease. *Hum Mol Genet.* 1993;2(5):545-8
89. Ruggeri ZM, Mendolicchio GL. Adhesion mechanisms in platelet function. *Circ Res.* 2007;100(12):1673-85
90. Fujimura Y, Titani K, Holland LZ, Russell SR, Roberts JR, Elder JH, Ruggeri ZM, Zimmerman TS. von Willebrand factor. A reduced and alkylated 52/48-kDa fragment beginning at amino acid residue 449 contains the domain interacting with platelet glycoprotein Ib. *J Biol Chem.* 1986;261(1):381-5
91. Sixma JJ, Schiphorst ME, Verweij CL, Pannekoek H. Effect of deletion of the A1 domain of von Willebrand factor on its binding to heparin, collagen and platelets in the presence of ristocetin. *Eur J Biochem.* 1991;196(2):369-75
92. Cruz MA, Yuan H, Lee JR, Wise RJ, Handin RI. Interaction of the von Willebrand factor (vWF) with collagen. Localization of the primary collagen-binding site by analysis of recombinant vWF a domain polypeptides. *J Biol Chem.* 1995;270(18):10822-7
93. Azuma H, Hayashi T, Dent JA, Ruggeri ZM, Ware J. Disulfide bond requirements for assembly of the platelet glycoprotein Ib-binding domain of von Willebrand factor. *J Biol Chem.* 1993;268(4):2821-7
94. Purvis AR, Gross J, Dang LT et al. Two Cys residues essential for von Willebrand factor multimer assembly in the Golgi. *Proc Natl Acad Sci USA.* 2007;104(40):15647-52
95. Lillicrap D. Genotype/phenotype association in von Willebrand disease: is the glass half full or empty? *J Thromb Haemost.* 2009;7(Suppl 1): 65-7
96. den Dunnen JT, Antonarakis SE. Mutation nomenclature extensions and suggestions to describe complex mutations: a discussion. *Hum Mutat.* 2000;15(1):7-12
97. Goodeve AC, Eikenboom JC, Ginsburg D et al. A standard nomenclature for von Willebrand factor gene mutations and polymorphisms. On behalf of the ISTH SSC Subcommittee on von Willebrand factor. *Thromb Haemost.* 2001;85(5):929-31

References

98. Ho SN, Hunt HD, Horton RM et al. Site-directed mutagenesis by overlap extension using the polymerase chain reaction. *Gene*. 1989;77(1):51-9 J K Pullen, L R Pease
99. James PD, O'Brien LA, Hegadorn CA et al. A novel type 2A von Willebrand factor mutation located at the last nucleotide of exon 26 (3538G>A) causes skipping of 2 nonadjacent exons. *Blood*. 2004;104(9):2739-45
100. Zuker M. Mfold web server for nucleic acid folding and hybridization prediction. *Nucleic Acids Res*. 2003;31(13):3406-15
101. Delibato E, Gattuso A, Minucci A et al. PCR experion automated electrophoresis system to detect *Listeria monocytogenes* in foods. *J Sep Sci*. 2009;32(21):3817-21
102. Berkowitz SD, Dent J, Roberts J et al. Epitope mapping of the von Willebrand factor subunit distinguishes fragments present in normal and type IIA von Willebrand disease from those generated by plasmin. *J Clin Invest*. 1987;79(2):524-31
103. Casonato A, De Marco L, Gallinaro L et al. Altered von Willebrand factor subunit proteolysis and multimer processing associated with the Cys2362Phe mutation in the B2 domain. *Thromb Haemost*. 2007;97(4):527-33
104. Federici AB, Canciani MT, Forza I et al. A sensitive ristocetin co-factor activity assay with recombinant glycoprotein Ibalpha for the diagnosis of patients with low von Willebrand factor levels. *Haematologica*. 2004;89(1):77-85
105. Ruggeri ZM, Zimmerman TS. Variant von Willebrand's disease: characterization of two subtypes by analysis of multimeric composition of factor VIII/von Willebrand factor in plasma and platelets. *J Clin Invest*. 1980;65(6):1318-25
106. Budde U, Pieconka A, Will K, Schneppenheim R. Laboratory testing for von Willebrand disease: contribution of multimer analysis to diagnosis and classification. *Semin Thromb Hemost*. 2006;32(5):514-21
107. Adinolfi E, Callegari MG, Ferrari D et al. Basal activation of the P2X7 ATP receptor elevates mitochondrial calcium and potential, increases cellular ATP levels, and promotes serum-independent growth. *Mol Biol Cell*. 2005;16(7):3260-72

References

108. Schwarz HP, Schlokot U, Mitterer A et al. Recombinant von Willebrand factor-insight into structure and function through infusion studies in animals with severe von Willebrand disease. *Semin Thromb Hemost.* 2002;28(2):215-26
109. Turecek PL, Varadi K, Schlokot U, Pichler L, Dorner F, Schwarz HP. In vivo and in vitro processing of recombinant pro-von Willebrand factor. *Histochem Cell Biol.* 2002;117(2):123-9
110. Rosén H, Calafat J, Holmberg L, Olsson I. Sorting of Von Willebrand factor to lysosome-related granules of haematopoietic cells. *Biochem Biophys Res Commun.* 2004;315(3):671-8
111. Schneppenheim R, Budde U, Obser T et al. Expression and characterization of von Willebrand factor dimerization defects in different types of von Willebrand disease. *Blood.* 2001;97(7):2059-66
112. Hommais A, Stépanian A, Fressinaud E et al. Impaired dimerization of von Willebrand factor subunit due to mutation A2801D in the CK domain results in a recessive type 2A subtype IID von Willebrand disease. *Thromb Haemost.* 2006;95(5):776-81
113. Tjernberg P, Vos HL, Spaargaren-van Riel CC et al. Differential effects of the loss of intrachain-versus interchain-disulfide bonds in the cystine-knot domain of von Willebrand factor on the clinical phenotype of von Willebrand disease. *Thromb Haemost.* 2006;96(6):717-24
114. Eikenboom JC, Matsushita T, Reitsma PH et al. Dominant type 1 von Willebrand disease caused by mutated cysteine residues in the D3 domain of von Willebrand factor. *Blood.* 1996;88(7):2433-41
115. Bodó I, Katsumi A, Tuley EA, Eikenboom JC, Dong Z, Sadler JE. Type 1 von Willebrand disease mutation Cys1149Arg causes intracellular retention and degradation of heterodimers: a possible general mechanism for dominant mutations of oligomeric proteins. *Blood.* 2001;98(10):2973-9
116. Tjernberg P, Vos HL, Castaman G, Bertina RM, Eikenboom JCJ. Dimerization and multimerization defects of von Willebrand factor due to mutated cysteine residues. *J Thromb Haemost.* 2004;2(2):257-65.
117. Gonzalez-Alegre P, Bode N, Davidson BL, Paulson HL. Silencing primary dystonia: lentiviral-mediated RNA interference therapy for DYT1 dystonia. *J Neurosci.* 2005;25(45):10502-9

References

- 118.Hickerson RP, Smith FJD, Reeves RE et al. Single-nucleotide-specific siRNA targeting in a dominant-negative skin model. *J Invest Dermatol.* 2008;128(3):594-605
- 119.Mannucci PM, Federici AB, James AH, Kessler CM. Von Willebrand disease in the 21st century: current approaches and new challenges. *Haemophilia.* 2009;15(5):1154-8

ABSTRACT:

Understanding molecular mechanisms leading to the dominant inheritance of von Willebrand disease (VWD) would improve our knowledge on pathophysiological aspects underlying its high prevalence. We produced a cellular model of severe type 2 VWD, caused by an heterozygous deletion in the VWF gene, to investigate the altered biosynthesis. Co-expression of the VWF in-frame deleted cDNA (p.P1105_C1926delinsR) impaired wild type vector-driven protein secretion and function (VWF collagen-binding $1.9 \pm 0,5\%$ of wt), which mimicked the patient's phenotype.

Protein studies and cell immunostaining delineated the highly efficient dominant-negative mechanism. The deleted VWF was synthesized in large amounts and preferentially processed, and through a correctly encoded "cysteine knot" domain formed heterodimers and heterotetramers with wild type VWF. Impaired multimerization was associated with reduced amounts of VWF in late endosomes.

The key role of heterodimers as multimer terminators was further supported by introduction of the dimerization mutation C2773R in the deleted construct, which resulted in a quantitative defect with normal multimer size. Targeting the mRNA breakpoint by siRNA selectively inhibited the in-frame deleted VWF expression, and restored secretion of functional VWF ($28.0 \pm 3.3\%$ of wt). This provided a novel tool to explore mutation-specific gene therapy in a severe form of dominant VWD.

RIASSUNTO IN ITALIANO:

La comprensione dei meccanismi molecolari che determinano l'ereditarietà di tipo dominante della malattia di von Willebrand aumenta, di conseguenza, la conoscenza degli aspetti patofisiologici che determinano la sua prevalenza. Abbiamo prodotto un modello cellulare di un severo caso di malattia di von Willebrand tipo 2, causato da una delezione presente in eterozigosi nel gene del fattore di von Willebrand (VWF), per studiare la biosintesi della proteina mutata. La co-espressione del cDNA contenente la delezione "in-frame" (p.P1105_C1926delinsR) diminuisce la secrezione e la funzionalità della proteina derivante dall'espressione del vettore "wild type" (VWF:CB $1.9 \pm 0,5\%$ of wt), e mima il fenotipo del paziente. Gli studi condotti a livello proteico e gli esperimenti di immunofluorescenza indicano un meccanismo dominante-negativo particolarmente efficiente. La proteina deleta è sintetizzata in gran quantità ed è preferenzialmente processata e, attraverso il dominio "cysteine knot" correttamente codificato forma eterodimeri ed eterotetrameri con proteine VWF "wild type". La compromissione del meccanismo di multimerizzazione è associata a una ridotta quantità di proteina VWF negli endosomi ("late endosomes").

Il ruolo chiave degli eterodimeri come terminatori della multimerizzazione è inoltre supportato dall'effetto dovuto all'introduzione della mutazione C2773R nel costrutto deleta, la quale determina un difetto quantitativo in cui però i multimeri hanno dimensioni normali.

Utilizzando siRNA diretti contro il breakpoint è possibile silenziare selettivamente l'espressione della sola proteina VWF deleta, e ottenere un conseguente recupero dei livelli di VWF (VWF:CB $28.0 \pm 3.3\%$ of wt). Questo approccio è un esempio per esplorare meccanismi di terapia genica mutazione-specifica in severe forme di malattia di von Willebrand, potenzialmente applicabili ad altre malattie causate da mutazioni con lo stesso effetto dominante-negativo.

Curriculum vitae et studiorium

The author of this thesis was born in Ferrara (Italy) on July 23, 1981, and accomplished secondary education at the high school "Liceo Scientifico -A. Roiti-" in Ferrara. From 2000 to 2004 she was a student at the University of Ferrara, Biological science course, and graduated (bachelor degree -Laurea di Primo Livello-) cum laude with a thesis entitled "Cellular microparticles: role in the coagulation" wrote under the supervision of Prof. Francesco Bernardi. From 2004 to 2006 she was student at the same University and finally obtained the Biomolecular and Cellular Science Master Degree (Laurea Specialistica) cum laude with an experimental work on von Willebrand factor. In 2007 she entered a PhD program in Biochemistry, Molecular Biology and Biotechnology at the same University under the supervision of Dr. Mirko Pinotti and Prof. Francesco Bernardi and she had the opportunity to study the molecular mechanism of a dominant-negative von Willebrand factor gene deletion and to propose a correction strategy based on siRNAs. Results described in this thesis were presented by the author at the last XXII Congress of the International Society on Thrombosis and Haemostasis, (Boston, USA -July 2009-) and she received the Young Investigator Award. Recently a manuscript containing most of these data has been submitted to Blood for publication.

Acknowledgement

I am deeply grateful to Prof. Francesco Bernardi and Dr. Mirko Pinotti for opening my mind to science and sharing their knowledge to me supporting my work through the years. I also thank all my colleagues for their patience and for many valuable advices they have given to me. I would like to acknowledge Prof. Raimondo De Cristofaro e Stefano Lancellotti -Catholic University of Rome- for their scientific help and kindness. This thesis would never have been possible without the constant support and help of my precious family and of my good and sincere friends.